ON THE SIMULATIONS OF CORRELATED NAKAGAMI-M FADING CHANNELS USING SUM –OF-SINUSOIDS METHOD

A Thesis Presented to the Faculty of Graduate School of

University of Missouri-Columbia

In Partial Fulfillment

Of the Requirements for the Degree of

Master of Science

By

Dhiraj Dilip Patil

Dr. Chengshan Xiao, Thesis Supervisor

December 20006

The undersigned, appointed by the dean of the Graduate School, have examined the [thesis] entitled

ON THE SIMULATIONS OF CORRELATED NAKAGAMI-M FADING CHANNELS USING SUM-OF-SINUSOIDS METHOD

presented by Dhiraj Dilip Patil, a candidate for the degree of MASTER OF SCIENCE, and hereby certify that, in their opinion, it is worthy of acceptance.

Dr. Chengshan Xiao
Dr. Justin Legarsky
Dr. Haibin Lu

DEDICATION

..... Thanks, Family and Friends

ACKNOWLEDEMENTS

I would like to thank my research advisor Dr. Chengshan Xiao. Without his enthusiasm and inspiration, this work would not be possible. He not only suggested me research topic but also provided encouragement, sound advice and excellent teaching in timely manner, which helped me to achieve my goals. I would like to thank my parents and brother for their constant support throughout the duration of my graduate studies. I would like to thank all my close friends especially Amit Gandhi, who always have been very helpful throughout these years of a degree.

TABLE OF CONTENTS

TABLE OF FIGURES

LIST OF TABLES

LIST OF ABBREVATIONS

PDF:	Probability Density Function
CDF:	Cumulative Density Function
BER:	Bit Error Rate
S/N or SNR:	Signal to Noise ratio
T/R:	Transmitter/Receiver
RMS:	Root Mean Square
LCR:	Level Crossing Rate
AFD:	Average Fade Duration
dB:	Decibel

ABSTRACT

Signal Fading can drastically affect the performance of terrestrial communication systems. Fading caused by multipath propagation can degrade the bit-error-rate (BER) performance of a digital communication system resulting data loss or dropped calls in a cellular system. So it is essential to understand the nature of multipath fading phenomenon and how to anticipate when such phenomenon occurs in order to improve radio performance.

The Nakagami-m distribution has gained widespread application in the modeling of physical fading radio channels. The primary justification of the use of Nakagami-m fading model is its good fit to empirical fading data. It is versatile and through its parameter m, we can model signal fading conditions that range from severe to moderate, to light fading or no fading.

This research work discusses the generation of Nakagami-m fading samples from sum-of-sinusoids method in which Nakagami process is generated by taking square root of Gamma process. Gamma process itself can be realized using Gaussian processes. We have used Improved Jake's Model to characterize the low-pass Gaussian Processes. We also studied second order statistics e.g. ensemble autocorrelation of this simulator and essential properties like Level Crossing Rate and Average Fade Duration. It has been found that simulation and theoretical results have very good fit. Furthermore, we extended this methodology to n-branch vector Nakagami-m fading channel for diversity

reception. We have found excellent agreement of the simulation results to its theoretical counterparts.

CHAPTER 1

INTRODUCTION

1.1) Motivation

In the recent years, radio-engineering requirements have become more stringent and necessitate not only more detailed information on median signal intensity, but also much more exact knowledge on fading statistics in both ionospheric and tropospheric modes of propagation. Such circumstances demanded a large number of experiments and number of theoretical investigations to be performed. Field tests in a mobile environment are considerably more expensive and may require permission regulatory authorities. It is difficult to generate repeatable field test results due to random, uncontrollable nature of the mobile communication path. Atmospheric conditions and cost also play a key role in field test measurements. These limitations can be overcome by means of simulation.

A simulation is an imitation of some real phenomenon, state of affairs, or process. The act of simulating generally entails representing certain key characteristics or behaviors of a selected physical or abstract system. Simulation is used in many contexts, including the modeling of natural systems or human systems in order to gain insights into their functioning. Other contexts include simulation of technology for performance optimization. Simulation can be used to show eventual real effects of alternate conditions and courses of action.

Key issues in simulation include acquisition of valid source information about the referent, selection of key characteristics and behaviors, the use of simplifying approximations and assumptions within the simulation, and the fidelity and validity of simulations results.

The main motive to run simulations can be described

- Simulation as a technique: - Investigate the detailed dynamics of a system
- Simulation as a heuristic tool: - Develop hypothesis, models and theories.
- Simulation as a substitute for an experiment: - Perform numerical experiments
- Simulation as pedagogical tool: - Gain understanding of a process.

Approximations and assumptions are used extensively to simplify the simulation model. The most commonly used assumptions and approximations involve time invariance (stationarity) and linearization. While most practical systems, when observed over a long period of time and over a wide dynamic range of input signal, might exhibit time-varying and non-linear behavior. However they can be well approximated by linear and time-invariant models over short time intervals and for low signal levels [23].

Having discussed briefly why we need simulation, let's turn our attention to mobile radio channel and network simulators in the communication systems.

Mobile radio channel simulators thus, are essential for repeatable systems tests in the development, design or test laboratory. The Rayleigh or Nakagami fading simulator can be used to test the performance of radios in a mobile environment in the lab, without the need to perform measurements whilst actually mobile. The mobile fading simulation can also be if required be replicated, and the effects can be varied according to the 'velocity'

of the mobile receiver. This allows the comparison of the performance of different receivers under standardized conditions that would not normally be possible in actual mobile testing situations. In case of mobile radio channel simulator, important assumption is time invariance. It implies that over the simulation interval, system components and properties of signal do not change.

Network Fading Simulator can also be used for the performance analysis of different modulation-demodulation schemes. Typically random binary sequences are generated and modulated using the desired modulation schemes (e.g. QPSK, PSK etc). This binary sequence is then detected under the presence of additive white Gaussian noise and multiplication noise. This multiplicative noise typically has Rayleigh or Nakagami distribution and can be generated by network fading simulator. Thus, a plot of Bit Error Rate (BER) and signal to noise ration (S/N) can be obtained. This plot can be used to demonstrate well-known effect called flooring.

1.2) Problem Definition

The main objective of this work can be summarized below

1.) Design a sum-of-sinusoids method to generate correlated Nakagami fading environment

2.) Apply decomposition technique and using above method to generate probability density function of correlated diversity system for given covariance matrix and given fading parameters.

However, a brief history of wireless fading environment, analysis and the related research work material is discussed in order to maintain the continuity.

The organization of rest of the thesis is as follows. Chapter 2 briefly explains the fading environment, key features and various definitions used. Chapter 3 presents brief literature review of Nakagami fading channels and existing algorithms to generate of fading samples for different fading parameters. Chapter 4 is dedicated to sum-of-sinusoids method to generate correlated fading samples; higher order statistics including ensemble autocorrelation, level crossing rate and average fade duration. Chapter 5 discusses the application of the same method in case of diversity systems with given covariance matrix and fading parameters. The results of these two simulations have been discussed in chapter 6. The conclusion and scope of future work are discussed in chapter 7. Appendix of derivations is also provided.

CHAPTER 2

THEORETICAL BACKGROUND & DEFINITIONS

In this chapter, we will develop theoretical background, which inspired this work. We will discuss a typical multipath propagation path, multipath fading, and different types of multipath fading phenomenon briefly.

2.1) Multipath Propagation

A typical mobile radio communication environment including PCS and digital cellular transmission link consists of an elevated base station antenna or multiple antennas and a relatively short distance line-of-sight (LOS) propagation path, followed by many non LOS propagation paths and a mobile antenna or antennas mounted on a moving vehicle or more generally on the transmitter/receiver (T/R) or transceiver of the mobile or portable unit. In such an environment, the transmitted waves often do not reach the receiving antenna directly. Man-made or natural obstacles usually block the emitted electromagnetic waves. The received waves are a superimposition of waves coming from all the direction due to reflection, diffraction and scattering caused by obstacles. This effect is known as ***Multipath Propagation***.

Due to this effect, the received signal consists of an infinite sum of delayed, phase-shifted and attenuated replicas of transmitted signal. The superposition can be constructive or destructive depending upon the phase of each replica.

In addition to the Multipath propagation, Doppler Effect has an adverse effect on the transmission characteristics of the mobile radio channel. The ***Doppler Effect*** is the apparent change in frequency and wavelength of the wave perceived by an observer moving relative to the source of waves. Due to the movement of the vehicle, the Doppler Effect causes a frequency shift of each of the partial waves.

Even the smallest, slowest movement causes time variable multipath, thus random time variable signal reception. For example, assume user is sitting in a stationary vehicle in a parking lot, near a busy freeway. Although user is stationary, part of environment surrounding him is moving at a speed of 100 km/hr. The automobiles on freeway become "reflectors" of the radio signal. If during the transmission or reception, user is also moving (100km/hr), the randomly reflected signals vary at faster rate. The ***Doppler spread*** is a measure of the spectral broadening caused by the time rate of change of the mobile radio channel and is defined as the range of frequencies over which received Doppler spectrum is non-zero.

The following figure shows a typical multipath propagation environment.

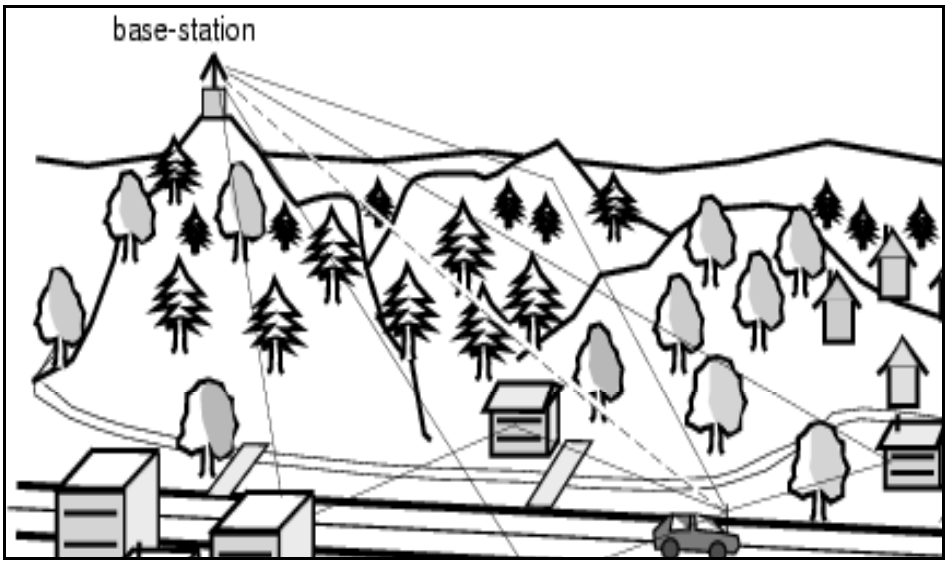

Figure 2.1: Typical Multipath Propagation Environment.

Besides Multipath Propagation, Multipath Fading, Shadowing and Path Loss characterize the radio propagation environment.

- Multipath propagation leads to the random fluctuations in amplitude and phase of the received signal due to the movement of receiver and/or the transmitter over a few wavelengths or short time duration. Depending upon the speed of the mobile unit fades of 30 to 40 db or more below the mean value of received signal have been observed. The phenomenon of rapid fluctuations of the received signal strength over short distance or short duration is called ***"small scale effect***".
- The ***'large scale'*** effects caused the received power to vary gradually due to signal attenuation determined by the geometry of the path profile in its entirety. This phenomenon is affected by prominent terrain contours (hills, mountains, trees, buildings, billboards etc.) between the transmitter and receiver. The receiver is often represented as being "shadowed". The statistics of large-scale fading provides a way of computing an estimate of path loss as a function of distance.

- **Shadowing**: The density of the obstacles between transmit and receive antennas depends very much on the physical environment. E.g. outdoor plains have very little by way of obstacles while indoor planes pose many obstacles. This randomness in the environment is captured by modeling the density of the obstacles and their absorption behavior as random numbers. The overall phenomenon is known as ***'Shadowing'.***

  The duration of shadow fades last for multiple seconds or minutes and hence occurs at much slower time-scale compared to multipath fading.

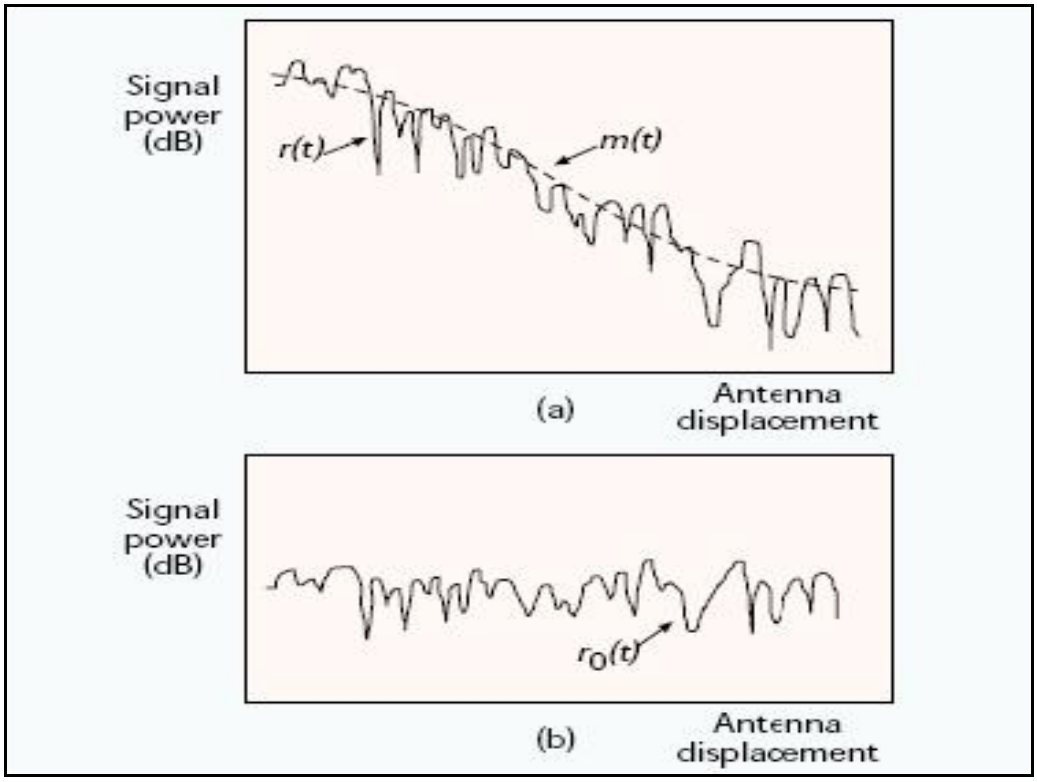

Figure 2.2: Large scale and Small scale fading.

The figure 2.2 illustrates the relationship between small-scale and large-scale fading. Small-scale fading superimposed on large-scale fading can be easily identified. The typical antenna displacement between the small-scale fading nulls is half wavelength. In

figure 2.2 b) large-scale fading m (t) has been removed in order to view small scale fading $r_0(t)$.

Path Loss models describe the signal attenuation between transmit and receive antennas as a function of propagation distance and other parameters. Some models can include many details of terrain profile to determine the attenuation.

The large -scale effects determine a power level averaged over an area of tens or hundreds of meters and therefore called the '***area-mean***' power. Shadowing introduces more additional fluctuations, so the local mean power fluctuates around area mean power. The 'local-mean' is averaged over a few tens of wavelengths, typically 40 wavelengths. This ensures that the rapid fluctuations of the received power caused by multipath effects are largely removed. The following figure shows the fading channel manifestations.

2.2) Time Dispersion Parameters

Along with Doppler spread, the term ***Coherence time*** is used to describe time varying nature of fading channel in a small-scale region. Coherence time is a statistical measure of time duration over which the channel impulse response is essential invariant. If the reciprocal bandwidth of the base-band signal is greater than the coherence time of the channel, then the channel will change during the transmission of the base-band message causing signal distortion. Coherence time and Doppler spread are inversely proportional.

Thus, Doppler spread and Coherence time together describe time varying nature of fading channel.

Time dispersive nature of channel is characterized by ***Delay spread*** and ***Coherence bandwidth.***

Coherence bandwidth is a statistical measure of the range of frequencies over, which channel can be considered “flat”. I.e. channel which passes all spectral components with approximately equal gain and linear phase. Delay spread is a natural phenomenon caused by reflected and scattered propagation paths in radio channel. RMS Delay spread and Coherence bandwidth are inversely proportional.

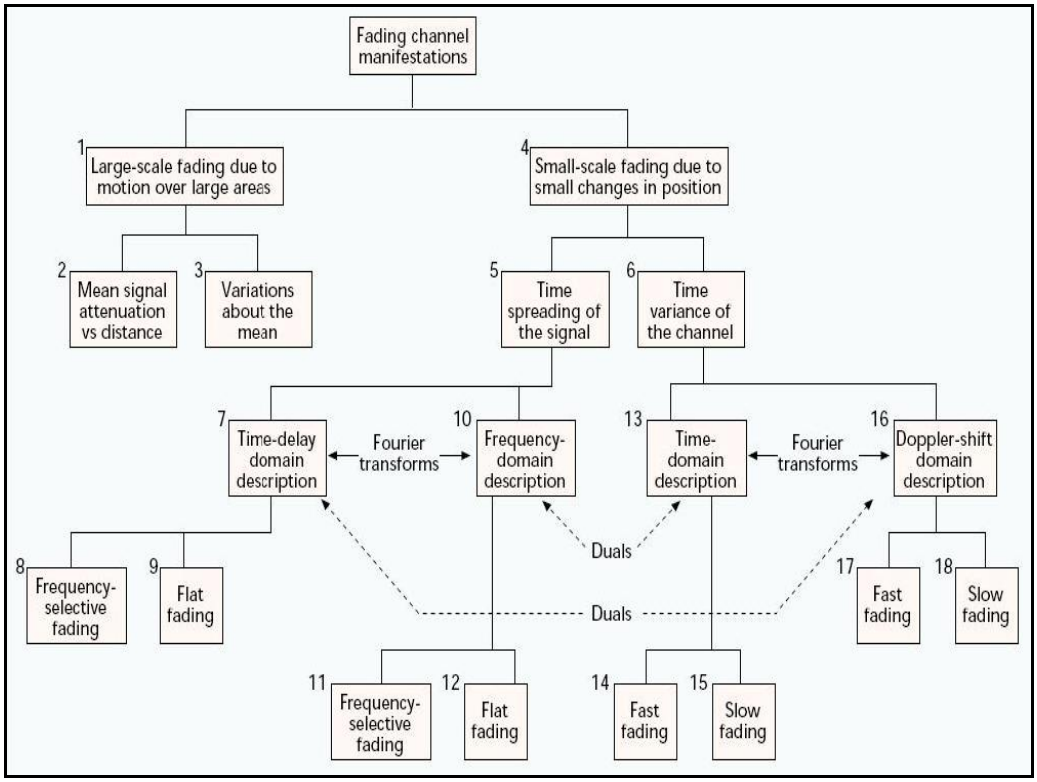

Figure 2.3: Fading Channel Manifestations

2.3) Multipath Fading

Multipath Fading is characterized by *envelope fading* (non-frequency-selective amplitude distribution), *Doppler Spread* (time selective or time variable random phase noise) and *time-delay spread* (variable propagation distance of reflected signals cause time variations in the reflected signals). These signals cause frequency selective fades. These phenomena are summarized in figure 2.3.

Doppler Spread is defined as the spectral width of a received signal when a single sinusoidal carrier is transmitted through the multipath channel. If a carrier wave (an unmodulated sinusoidal tone) having a radio frequency ' f_c ', then because of Doppler spread ' f_d ', we receive a smeared signal spectrum with spectral components between ' $f_c - f_d$ ' and ' $f_c + f_d$ '. This effect may be interpreted as ***temporal decorrelation effect*** of random multipath faded channel and is known as '***time-selective fading'***. The effect of time-delay spread can be interpreted as a frequency-selective fading effect. This effect may cause severe distortions in the demodulated signals and can impose limits on the bit-error-ratio (BER) performance of high-speed wireless communication systems.

The following figure shows the relationship between different phenomena.

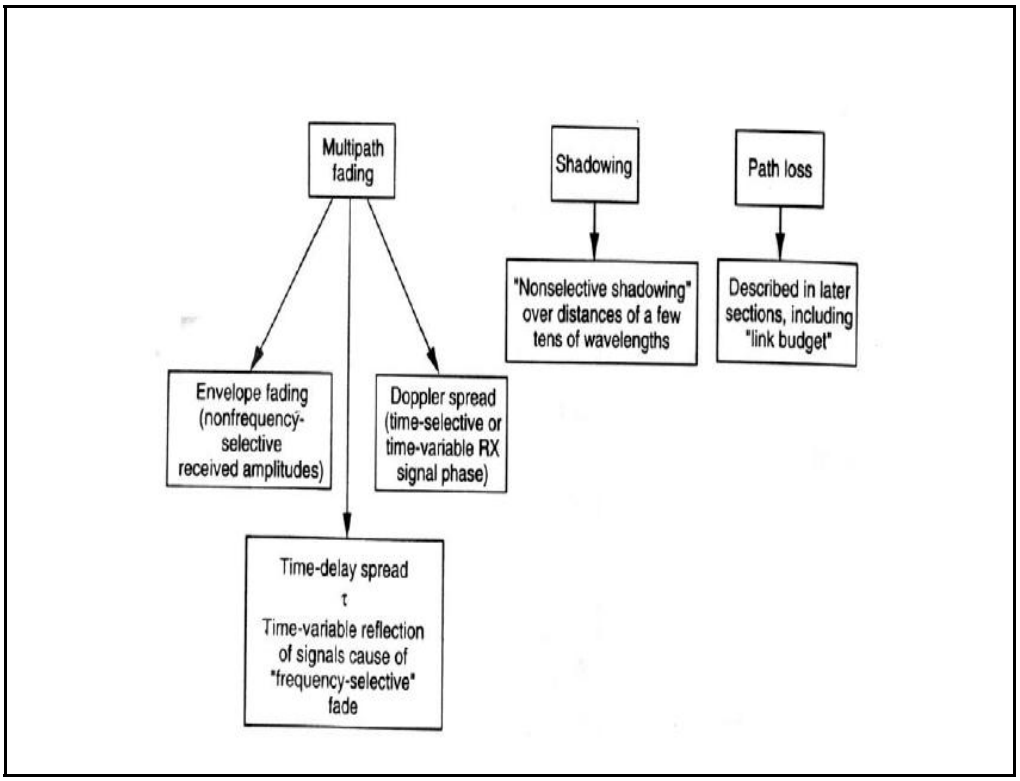

Figure 2.4: Multipath Fading, Shadowing and Path Loss Phenomenon

2.4) Types of Fading

In the literature, many models from the probability distribution function point of view have been discussed and researched. Out of these models, Rayleigh, Rician and Nakagami Fading models are most widely used. We will now discuss these models in brief [5].

2.4.1) Rayleigh Fading

Rayleigh fading is caused by multipath reception. The mobile antenna receives a large number of, say N, reflected and scattered replicas of same signal. Because of constructive

and destructive interference, the instantaneous received power seen by mobile antenna becomes a random variable, dependent upon the location of the antenna. Let's discuss the basic mechanisms of mobile reception. In case of an unmodulated carrier, the transmitted signal is given by the following equation.

$$S(t) = \cos(w_c t + \psi)$$

2.4.1.1) Effect of Motion

Let the n-th reflected wave has with an amplitude c_n and phase ϕ_n arrive at an angle α_n relative to the direction of motion of mobile antenna.

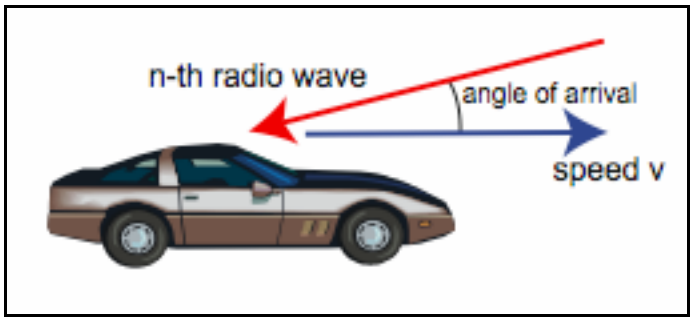

Figure 2.5: Angle of Arrival and position of moving vehicle

The Doppler shift of this wave is given by

$$\Delta f_n = \frac{v}{\lambda} \cos \alpha_n$$

Where v is the speed of mobile antenna and α_n is the angle of arrival.

2.4.1.2) Phasor Representation

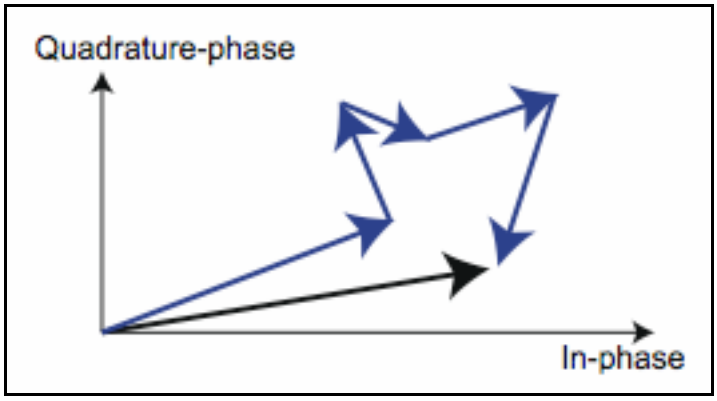

Figure 2.6: Phasor diagram of scattered waves (blue) and resultant Rayleigh fading envelope (black)

The received unmodulated signal r (t) can be expressed as

$$r(t) = \sum_{n=1}^{N} c_n \cos[2\pi(f_c + \Delta f_n)t + (\psi + \phi_n)]$$

The inphase-quadtrature representation is given by

$$r(t) = I(t)\cos(w_c t) - Q(t)\sin(w_c t)$$

Inphase and quadrature components of received signal are given by the following equations respectively.

$$I(t) = \sum_{n=1}^{N} c_n \cos(\frac{2\pi f_c t}{c} + \psi + \phi_n)$$

$$Q(t) = \sum_{n=1}^{N} c_n \sin(\frac{2\pi f_c t}{c} + \psi + \phi_n)$$

Provided that N is sufficiently large and all c_n are equal, then by ***central limit theorem,*** then I (t) and Q (t) can be shown as zero-mean stationary Gaussian processes.

2.4.1.3) Probability Distribution Function

If we express r (t) as: -

$$r(t) = R(t)\cos[2\pi f_c t + \theta(t)]$$

Then probability distribution function of amplitude and phase are given by respectively.

$$p(R) = \frac{R}{\sigma^2}\exp(-\frac{R^2}{2\sigma^2}) \qquad R \geq 0$$

$$p(\theta) = \frac{1}{2\pi} \qquad -\pi \leq \theta \leq \pi$$

The preceding equations show that received signal has Rayleigh distributed envelope R (t) and a uniformly distributed phase $\theta(t)$.

2.4.2) Rician Fading

Rician fading is similar to Rayleigh fading except for the fact that there exists a strong line-of-sight component along with reflected waves. Redefined Rician models also consider

- That the dominant component can be a Phasor sum of two or more dominant components. E.g. the line-of-sight, plus a ground reflection. This combined signal is then mostly treated as a deterministic process.

- That the dominant wave can be subjected to the shadow attenuation. This is a popular assumption in the modeling of satellite channels.

Besides the dominant component, mobile antenna receives a large number of reflected and scattered waves.

2.4.2.1) Phasor Representation

The following diagram shows the Phasor representation of Rician fading phenomenon.

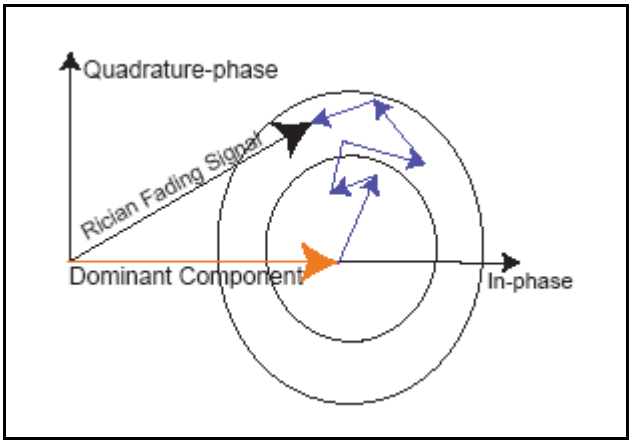

Figure 2.7: Phasor diagram of scattered waves (blue) dominant component (orange) and resultant Rician Fading Envelope (black)

2.4.2.2) Probability Density Function

In order to obtain the probability density function of signal amplitude we observe random processes I (t) and Q (t) at one particular time instant t_0 . If the number of scattered waves are sufficiently large and are independent and identically distributed, then by central limit

theorem, I (t_0) and Q (t_0) are zero-mean stationary Gaussian processes. But due to the deterministic dominant term, it has no longer zero mean. Transformation of variables show that the amplitude and phase have joint PDF

$$f_{p,\phi}(p,\phi) = \frac{\rho}{2\pi\sigma^2}\exp\{-\frac{\rho^2 + C^2 - 2\rho\cos\phi}{2\sigma^2}\}$$

Here, σ^2 is local-mean scattered power and $\frac{C^2}{2}$ is power of the dominant component.

The PDF of the amplitude can be found as

$$f_\rho(\rho) = \int_{-\pi}^{\pi} f_{\rho,\phi}(\rho,\phi)d\phi$$

$$= f_\rho(\rho) = \frac{\rho}{\sigma^2}\exp\{-\frac{\rho^2 + C^2}{2\sigma^2}\} I_0(\frac{\rho C}{\sigma^2})$$

Where I_0 is modified Bessel function of First kind and zero order, defined as

$$I_0(x) = \frac{1}{2\pi}\int_{-\pi}^{\pi} \exp(-x\cos\phi)d\phi$$

2.4.2.3) Rician Factor

The Rician factor K is defined as the ratio of signal power in dominant component to the (local-mean) scattered power.

Thus $K = \frac{DirectPower}{ScatteredPower} = \frac{C^2/2}{\sigma^2}$

2.4.3) Nakagami Fading

The Nakagami Distribution described the magnitude of the received envelope by the distribution

$$p(r) = \frac{2}{\Gamma(m)}\left(\frac{m}{\Omega_p}\right)^m r^{2m-1} \exp\{-\frac{mr^2}{\Omega_p}\} \qquad r \geq 0, \Omega \geq 0 \qquad m \geq \frac{1}{2}$$

$\Omega_p = E\left(r^2\right)$ Is an instantaneous power.

$m = \frac{E(r^2)}{\text{var}(r^2)}$ Is a fading figure or shape factor.

Nakagami Fading occurs for multipath scattering with relatively larger time-delay spreads, with different clusters of reflected waves. Within any one cluster, the phases of individual reflected waves are random, but the time delays are approximately equal for all the waves. As a result the envelope of each cluster signal is Rayleigh Distributed. The average time delay is assumed to differ between the clusters. If the delay times are significantly exceed the bit period of digital link, the different clusters produce serious intersymbol interference.

The following are the facts about Nakagami Fading.

- If the envelope is Nakagami Distributed, the corresponding power is Gamma distributed.
- The parameter ‘m’ is called fading figure or shape factor and denotes the severity of fading.

- In the special case m=1, Rayleigh fading is recovered, with an exponentially distributed instantaneous power.
- For m > 1, the fluctuations of the signal strength are reduced as compared to Rayleigh Fading.
- For m=0.5, it becomes one-sided Gaussian distribution.
- For m=∞, the distribution becomes impulse. I.e. no fading.
- The sum of multiple independent and identically distributed Rayleigh-fading signals has Nakagami Distributed signal amplitude.
- The Rician and Nakagami model behave approximately equivalently near their mean value. While this may be true for main body of the probability density, it becomes highly inaccurate for tails. As the outage mainly occurs during the deep fades, these quality measures are mainly determined by the tail of the probability density function. (For the probability to receive less power).

The Rician distribution can be closely approximated by using following relation between Rice Factor 'K' and Nakagami Shape Factor 'm'.

$$K = \frac{\sqrt{m^2 - m}}{m - \sqrt{m^2 - m}} \qquad m > 1$$

$$m = \frac{(K+1)^2}{(2K+1)}$$

Since the Rice distribution contains a Bessel function while the Nakagami distribution does not, the Nakagami distribution offers closed form analytical expressions, which are otherwise difficult to achieve.

2.5) Other Topics Pertaining to Nakagami-m Distribution

In order to design any simulator for fading model, it is necessary to study its correlation and higher order statistics. It provides the knowledge about the behavior of simulator for different parameters. The Probability Density Function (PDF) and Cumulative Density Function (CDF) are mainly known as first-order characteristics and can only be used to obtain static metrics associated with the channel, such as the Bit Error Rate (BER). The two quantities, Level Crossing Rate (LCR) and Average Fade Duration (AFD) statistically characterize a fading communication channel.

2.5.1) Definitions and General Formulae

2.5.1.1) Level Crossing Rate (LCR)

Level Crossing Rate is defined as the number of times per unit duration that the envelope of a fading channel crosses a given value in the negative direction.

2.5.1.2) Average Fade Duration (AFD)

Average Fade Duration corresponds to the average length of time the envelope remains under the threshold value once it crosses it in the negative direction.

These quantities reflect correlation properties, and thus the second-order statistics, of a fading channel.

Denoting time derivative the envelope r as R' and Level Crossing Rate as R, the LCR occurring at a certain level 'R' is defined as

$$N_R = \int_0^\infty r' \, p(r', r = R) dr'$$

Similarly Average Fade Duration can be defined as

$$T_R = \frac{prob(r \le R)}{N_R}$$

$$T_R = \frac{F_R(r)}{N_R(r)}$$

Where $F_R(r) = \int_0^r P_R(\alpha) d\alpha$ is the characteristic function of channel.

The analysis of LCR and AFD enables one to get the statistics of burst errors occurring on fading channel. This statistics provides useful information for the design of the error-correcting codes, which are complicated by the presence of error bursts. Interleaver size can be optimized based on such statistics. Interleaving is an operation of spreading burst errors into random errors. Further, LCR and AFD have found a variety of applications in the modeling and design of wireless communication systems, such as the finite-state Markov modeling of fading channels, the analysis of hand-off algorithms and the estimation of packet error rates.

CHAPTER 3

LITERATURE REVIEW

In the last chapter we have discussed the fundamentals of a typical wireless channels and studied few definitions. We will discuss the brief background of Nakagami-m distribution and generation techniques available in the literature.

3.1) Theory of Nakagami Fading

The first work of researching and developing of digital mobile communication system is to understand mobile channel characteristics itself. As we have seen in second chapter, Rayleigh and Rician fading models have been widely used to simulate small scale fading environments over decades. [1] States that Rayleigh fading falls short in describing long-distance fading effects with sufficient accuracy. M. Nakagami observed this fact and then formulated a parametric gamma function to describe his large-scale experiments on rapid fading in high frequency long-distance propagation. Although empirical, the formula is rather elegant and has proven useful.

The form of Nakagami-m distribution is given below.

$$p(r) = \frac{2}{\Gamma(m)}\left(\frac{m}{\Omega_p}\right)^m r^{2m-1} \exp\{-\frac{mr^2}{\Omega_p}\} \qquad m \geq \frac{1}{2}$$

$\Omega_p = E\left(r^2\right)$: -Instantaneous power.

$m = \frac{E(r^2)}{\text{var}(r^2)}$: -Fading figure or shape factor.

In addition to the m-distribution, the following two compact forms of distributions,

$$p(R) = \frac{2R}{\sigma}\exp(-\frac{R^2 + R_0^2}{\sigma})I_0(\frac{2RR_0}{\sigma})$$

$$p(R) = \frac{2R}{\alpha\beta}\exp\{-(\frac{R^2}{2})(\frac{1}{\alpha} + \frac{1}{\beta})\}I_0[\frac{R^2}{2}(\frac{1}{\beta} - \frac{1}{\alpha})]$$

Presented by Nakagami (1940) and by Nakagami and Sasaki (1942) respectively. The former named "n-distribution" is frequently used in radio engineering and latter, named "q-distribution", also appears in communication problems. More recently, (Nakagami, Wada, Fujimura, 1953) showed that the m-distribution is a more general solution with good approximation to the random vector problem. At the same time it was also shown that m-distribution includes in particular manner the two distributions stated above. Also, the mutual dependencies among their parameters were fully investigated, when m-distribution and the other distributions were fully transformed.

3.1.1) Discussion of Nakagami Probability Density Function

In order to better understand the Nakagami-m probability distribution function, it is important to understand the derivation of it. [1] Provides the details of the Nakagami-m formula.

3.1.1.1) Outline of the Original Derivation

A) Time Interval of Observation

In order to observe rapid fading alone, the length of the observation of interval should be chosen carefully, because the effect of small fading will be more predominant for too long time intervals. The statistical meaning becomes ambiguous for too short time intervals. The length of time intervals depends upon various factors such as frequency, propagation path. [1] States that the optimum time interval was found out to be three to seven minutes.

B) Apparatus and Observed waves

A vertical antenna, about 1.5m long was used, the output of which after amplification, logarithmic compression and envelope detection was applied to the deflection plates of CR tube. The functional forms of distributions of the results were determined as below.

$$p'(x) = \exp\{m(1+\frac{2x}{M} - e^{\frac{2x}{M}})\}$$ Where x is the signal intensity in dB (3.1)

Upon the normalization of this equation, we get

$$p(x) = \frac{2m^m}{M\Gamma(m)} \exp\{m(\frac{2x}{M} - e^{\frac{2x}{M}}\} = \mathrm{M}_x(x,m,0) \quad (3.2)$$

Using the transformation, $e^{\frac{x}{M}} = X = \frac{R}{\sqrt{\Omega}}$ where $\Omega = \overline{R^2}$ time average of square of intensity R, we get

$$p(X) = \frac{2m^m}{\Gamma(m)} X^{2m-1} e^{-mX^2} = \mathrm{M}_x(X,m,1) \quad (3.3)$$

$$p(R) = \frac{2m^m}{\Gamma(m)\Omega^m} R^{2m-1} e^{-(\frac{m}{\Omega})R^2} = \mathrm{M}_x(X,m,\Omega) \quad (3.4)$$

This is Nakagami-m distribution formula, includes both the Rayleigh distribution and one-sided Gaussian distribution as special cases of m=1 and m=0.5 respectively.

Note: - While Nakagami PDF has many attractive features, there is still no widely accepted general and efficient way of simulating a correlated Nakagami fading channel. This is partly due the fact that no temporal autocorrelation function was specified for the Nakagami PDF when it was proposed.

3.1.1.2) Properties of m-distribution

Now, let's discuss basic properties of m-distribution. The main results are formulated below. The exact details can be found in reference [1].

A) Referring to the equation (3.4), the distribution has maximum value at x=0 or $R = \sqrt{\Omega}$

$$p(0) = \frac{1}{M}\sqrt{\frac{2m}{\pi}} \qquad \text{(m large)}$$

B) When x<= M in equation (3.8), $\mathrm{M}_x(x, m, 0)$ approaches form of ***log-normal distribution.***

$$p(x) \approx \frac{1}{M}\sqrt{\frac{2m}{\pi}} e^{-2m(\frac{x}{M})^2}$$

3.2) Generation of Nakagami Signals

Unlike the generation of Rayleigh fading signals, the generation of Nakagami fading signals is different. Typically Rayleigh signals can be generated from two low- pass Gaussian processes i.e. in-phase and quadrature components and their magnitude follows Rayleigh distribution. However it is possible that the fading becomes more severe than Rayleigh fading as a result high variability in HF channels. As stated above, this fact was observed by Nakagami and the results of his channel measurements for some long-distance HF communication links showed that the m-distribution in the range of $0.5 \le m < 1$ is useful for modeling the fading characteristics of an HF channel when fading is more severe than Rayleigh fading. Note that the Rayleigh distribution is a special case of m-distribution when m=1.

Let's discuss the various methods researched best to my knowledge to generate correlated and uncorrelated Nakagami-m fading waveforms.

3.2.1) Generation of Correlated Nakagami Fading Signals

It is well known that Nakagami random variable is a square root of a gamma process and a gamma process itself can be realized from Gaussian random variable. Ertel and Reed [10] designed the method of generating tow correlated Rayleigh fading envelops of equal power. The idea used here is to exploit the fact that the envelope of a complex Gaussian variable follows Rayleigh distribution. The authors therefore were able to correlate the cross-correlation of these Rayleigh envelopes to their counterpart for the corresponding complex Gaussian variables. Until this period, there was no general technique available

to simulate Nakagami fading environment. Reference [2] uses a decomposition principle for representing a gamma vector as a direct sum of independent vectors. A set of independent vectors itself can be obtained from a set of correlated Gaussian vectors. The limitation of this method is all branches assume equal fading parameter. This drawback was addressed in reference [11], which offers more realistic model that allows arbitrary fading parameters, branch power and correlation matrix. The author derived a generic characteristic function of correlated Nakagami powered signals allowing all parameters to be arbitrary. [13] Provides a new algorithm to generate Nakagami-m random samples for arbitrary values of m, whereas the author claims that the previous generation methods are restricted to values of m between 0 and 1 and integer and half-integer values of m. Finally, [14] proposed a Nakagami-m fading simulator by incorporating pop's architecture. They also proposed modified version to generate uncorrelated Nakagami-m fading waveforms through orthogonal walsh-hadmard code words. Original Jake's model lacks the property of wide sense stationary. WSS can be achieved by inserting random phase in low frequency oscillators.

3.2.2) Generation of Nakagami Signals for m < 1

In the design of HF communication system, the system designer may want to ensure that the performance of the communication system is satisfactory not only in a Rayleigh fading environment but also in an environment characterized by more severe than Rayleigh fading. The care must be taken while investigating fading phenomenon when m<1. This represents more severe fading conditions than Rayleigh fading. To simulate Nakagami fading channels for m < 1, one needs to generate complex random process that

fits a given Doppler spectrum. Although there are many methods available to simulate Rayleigh fading channels, techniques for simulating an m-fading channel with m < 1 are relatively few. According to [12], complex random processes used for simulating an m-fading channel, m< 1, can be expressed as a product of a complex Gaussian process and a square root beta process. The square root beta process can be realized by a nonlinear transformation of complex Gaussian process. The advantage of this method is one can avoid the difficult task of determining amplitude values for sinusoids. Although this method is efficient, the algorithm developed is too complex to realize. [13] Offers a simple solution to generate fading samples for m< 1.

3.2.3) Generation of Uncorrelated Nakagami Signals

However, the generation of independent Nakagami-m random variates is also an important problem with many practical applications. For example, the generation of independent Nakagami-m random variables is required to simulate the performance of channel estimators [6]-[8] and diverse systems operating in very slow Nakagami-m fading channels. Other techniques are use method of rejection to generate samples of Nakagami distribution. Reference [9] gives detailed description and proof of rejection method. This is a simple algorithm to generate uncorrelated Nakagami-m samples. The acceptance-rejection method is well known. The challenge in this method is to find the hat function that is both easy to compute and close enough to scaled desired probability density function. The regions $0.5 \le m < 1$ and $m \ge 1$ represent fundamentally different fading scenarios and should be carefully handled. Suppose we need to generate samples of X with Nakagami-m distribution. $f_x(X)$. As mentioned above we would look for hat

function $f_W(x)$, that is easy to generate and which has the property that there exists some constant C, such that

$$Cf_W(x) \geq f_X(x) \qquad \text{For all x}$$

Once a suitable $f_W(x)$ has been found, generating samples of Nakagami fading samples is relatively easy. The efficiency of this method is given by 1/C.

3.3) Higher Order Statistics of Nakagami-m Distribution

While Nakagami PDF has many attractive features, there is still no widely accepted general and efficient way if simulating a correlated Nakagami fading channel. This is partly due to the fact that no temporal correlation was specified when it was proposed. Therefore most simulators need to make certain assumptions in order to model temporal autocorrelation of a Nakagami fading channel. Some analytical work has been carried out with respect to higher order statistics.

[15] Provides the exact formula for LCR and AFD for $m = \frac{n}{2}$ where n is non-negative integer value. But the simulation has shown that results agree with theoretical results for any m. Analytical LCR and AFD for diversity techniques have been thoroughly considered in [16]. The LCR and AFD expressions are rearranged such that it can be expressed as the product of the PDF of received signal and an integral involving the conditional derivative of this signal. Depending upon different diversity schemes, first term can be found in the literature or can be derived. The conditional PDF in second term can found by examining the expression for derivative of received sign. We have seen the

brief background research work being carried best to my knowledge. Let's state the idea behind the research problem in next section.

3.4) Idea Behind research Problem

Having discussed the brief background in this area, there are very few articles in the literature based of sum of sinusoids method for the generation of correlated Nakagami fading signals. The references [2] and [14] motivated work behind this research.

In chapter 4, the details of sum of sinusoids method will be introduced. We will briefly discuss the statistical properties of the proposed simulator and will study higher order statistics including level crossing rate and average fade duration of fading signals. Based on the principle used in this chapter 4, we will see an application of this method to generate probability density function for 4 branch diversity system with given covariance matrix and given fading parameter in chapter 5. The detailed analysis and results are discussed in chapter 6.

CHAPTER 4

SUM-OF-SINUSOIDS MODEL FOR NAKAGAMI-m FADING CHANNELS

4.1) Preliminaries

The well-known mathematical model due to Clarke and its simplified simulation model by Jake's have been widely used to simulate Rayleigh fading channels for past four decades. However, Jakes presumed a correlation among phase shifts conveniently. Therefore Jake's model is not Wide Sense Stationary property. However, Nakagami-m distribution has gained attention recently because it can model signals in severe, moderate, light, and no fading environment by adjusting its shape parameter, m. Actually sum of mutually exclusive Hoyt and Rician models is the Nakagami-m distribution. Let's briefly take look at basic models, which lead to Nakagami fading model.

4.1.1) Clarke's Rayleigh Fading Model

The base-band signal of the normalized Clarke's two-dimensional (2-D) isotropic scattering Rayleigh fading model is given by [18] as

$$g(t) = \frac{1}{\sqrt{N}} \sum_{n=1}^{N} \exp[j(w_d t \cos \alpha_n + \phi_n)] \qquad (4.1)$$

Where N is number of propagation paths, w_d is the maximum angular Doppler frequency, α_n, ϕ_n are the angel of arrival and initial phase of nth propagation path respectively. Both α_n, ϕ_n are uniformly distributed over $[-\pi, \pi]$.

According to Central Limit Theorem, the real part, $g_c(t) = \mathrm{Re}[g(t)]$ and the imaginary part $g_s(t) = \mathrm{Im}[g(t)]$ can be approximated as Gaussian Processes for large number of N. However, the fading statistics for finite number of N of Clarke's model are not available in the literature.

The autocorrelation and cross-correlation function of the quadrature components and the autocorrelation of the complex envelope and the squared envelope of fading signal are given below.

$$R_{gcgc}(\tau) = R_{gsgs}(\tau) = \frac{1}{2} J_0(w_d \tau) \tag{4.2}$$

$$R_{gcgs}(\tau) = R_{gsgc}(\tau) = 0 \tag{4.3}$$

$$R_{gg}(\tau) = J_0(w_d \tau) \tag{4.4}$$

$$R_{|g|^2|g|^2}(\tau) = 1 + J_0^2(w_d \tau) - \frac{J_0^2(w_d \tau)}{N} \tag{4.5}$$

Where $J_0(.)$ is the zero-order Bessel function of first kind. [19].

4.1.2) Pop-Beaulieu Simulator

Based on Clarke's model given by (4.1), Pop-Beaulieu proposed a class of wide sense stationary Rayleigh fading simulator by setting $\alpha_n = \frac{2\pi n}{N}$ in g (t)

The low-pass fading processes take form

$$X_c(t) = \frac{1}{\sqrt{N}} \sum_{n=1}^{N} \cos(w_d t \cos\frac{2\pi n}{N} + \phi_n) \tag{4.6}$$

$$X_s(t) = \frac{1}{\sqrt{N}} \sum_{n=1}^{N} \sin(w_d t \cos\frac{2\pi n}{N} + \phi_n) \tag{4.7}$$

However they mentioned that even though their simulator is wide sense stationary, it might not model higher-order statistical properties.

The autocorrelation and cross-correlation function of the quadrature components and the autocorrelation of the complex envelope and the squared envelope of fading signal are given below.

$$R_{XcXc}(\tau) = R_{XsXs}(\tau) = \frac{1}{2N} \sum_{n=1}^{N} \cos(w_d \tau \cos\frac{2\pi n}{N}) \tag{4.8}$$

$$R_{XcXs}(\tau) = -R_{XsXc}(\tau) = \frac{1}{2N} \sum_{n=1}^{N} \sin(w_d \tau \cos\frac{2\pi n}{N}) \tag{4.9}$$

$$R_{XX}(\tau) = 2R_{XcXc}(\tau) + j2R_{XcXs}(\tau) \tag{4.10}$$

$$R_{|X|^2|X|^2}(\tau) = 1 + 4R^2{}_{XcXc}(\tau) + 4R^2{}_{XcXs}(\tau) - \frac{1}{N} \tag{4.11}$$

It has been found that the second order statistics of this modified model with N = ∞ are same as the desired ones of the original Clarke's model.

4.1.3) Improved Rayleigh Fading Model

Based on Clarke's model and the Pop-Bealieu Simulator, An improved simulation model is given by an Improved Rayleigh Fading Simulator.

The normalized low-pass fading process of improved sum-of-sinusoids is given by

$$Y_c(t) = \frac{1}{\sqrt{N}} \sum_{n=1}^{N} \cos(w_d t \cos\alpha_n + \phi_n) \tag{4.12}$$

$$Y_s(t) = \frac{1}{\sqrt{N}} \sum_{n=1}^{N} \sin(w_d t \cos\alpha_n + \phi_n) \tag{4.13}$$

With $\alpha_n = \frac{2\pi n + \theta_n}{N}$ n=1, 2, 3, 4…N and θ_n and ϕ_n are uniformly distributed over $[-\pi, \pi]$ for all values of n.

We can note that this model differs from Clarke's model in that it forces the angle of arrival α_n between the intervals $\left[\frac{2\pi n - \pi}{N}, \frac{2\pi n + \pi}{N}\right]$. The important difference between this model and Pop-Beaulieu simulator is the introduction of random variables θ_n to the angle of arrival.

The autocorrelation and cross-correlation of quadrature components, and the autocorrelation function of the complex envelope and the squared envelope of fading signal Y (t) are given by following equations.

$$R_{YcYc}(\tau) = R_{YsYs}(\tau) = \frac{1}{2} J_0(w_d \tau) \tag{4.14}$$

$$R_{YcYs}(\tau) = R_{YsYc}(\tau) = 0 \tag{4.15}$$

$$R_{YY}(\tau) = J_0(w_d \tau) \tag{4.16}$$

$$R_{|Y|^2|Y|^2}(\tau) = 1 + J_0^2(w_d \tau) - f_c(w_d \tau, N) - f_s(w_d \tau, N) \tag{4.17}$$

Where

$$f_c(w_d \tau, N) = \sum_{n=1}^{N} \left[\frac{1}{2\pi} \int_{\frac{2\pi k - \pi}{N}}^{\frac{2\pi k + \pi}{N}} \cos(w_d \tau \cos\gamma) d\gamma \right]^2 \tag{4.18}$$

$$f_s(w_d \tau, N) = \sum_{n=1}^{N} \left[\frac{1}{2\pi} \int_{\frac{2\pi k - \pi}{N}}^{\frac{2\pi k + \pi}{N}} \sin(w_d \tau \cos\gamma) d\gamma \right]^2 \tag{4.19}$$

Comparing equations (4.2), (4.3) with (4.14), (4.15), we can easily see that first order statistics of improved Rayleigh fading simulator are similar to those of Pop-Beaulieu' simulator equations. However, second-order statistics are different and are given by (4.16) and (4.17).

4.2) Nakagami and Other Distributions

As seen in chapter 2, the Nakagami-m probability distribution function is given by following equation.

$$p_R(r) = \frac{2}{\Gamma(m)}\left(\frac{m}{\Omega_p}\right)^m r^{2m-1} \exp\{-\frac{mr^2}{\Omega_p}\} \qquad r \geq 0, \Omega \geq 0 \qquad m \geq \frac{1}{2} \tag{4.20}$$

Where $\Gamma(.)$ is a gamma function and $\Omega = E[z^2]$ is the second moment of R.

The shape parameter or fading figure m is defined as ratio of the moments and is given by

$$m = \frac{\Omega^2}{E\left[(R^2 - \Omega)\right]^2}$$

In order to understand sum-of-sinusoids method, let's review of relationships among important distribution functions i.e. normal, gamma and Nakagami.

4.2.1) Relationship between Gaussian, Gamma and Nakagami Random Variables

The Nakagami-m random processes Z can be obtained through the gamma random process G, by a mapping function $G = Z^2$.

We know that the Gamma distribution is the sum of a set of statistically independent and identically distributed central chi-square distributions.

A mapping form $\aleph = x^2$, where x is a normal distribution with zero mean and variance σ^2 characterizes the central chi-square distribution.

These relationships can be summarized as below.

$$X(0,\sigma^2) \text{------->} \aleph(m,\Omega) \text{------->} NK(m,\Omega)$$

Where X, $\aleph$ and NK are normal, chi-square and random variables.

The probability distribution function of central chi-square random variable is given by

$$p_\chi(\chi) = \frac{1}{\sqrt{2\pi\chi\sigma^2}} \exp(-\frac{\chi}{2\sigma^2}), \qquad \chi \geq 0 \tag{4.21}$$

With its characteristic function as

$$\Psi_\chi(jv) = (1 - jv2\sigma^2)^{-\frac{1}{2}} \tag{4.22}$$

It follows that the characteristic function of the central chi-square distribution with n-degrees of freedom, $U = \sum_{i=1}^{n} x_i^2$ with independently and identically distributed RV x_i, i=1, 2, 3…n is given by

$$\Psi_U(jv) = (1 - jv2\sigma^2)^{-\frac{n}{2}} \tag{4.23}$$

The inverse transform of this characteristic function yields its corresponding probability distribution function and is given by following equation.

$$p_U(u) = \frac{1}{\Gamma\left(\frac{n}{2}\right)\left(2\sigma^2\right)^{\frac{n}{2}}} u^{\frac{n}{2}-1} \exp\left\{-\frac{u}{2\sigma^2}\right\} \qquad u \geq 0 \tag{4.24}$$

The first moment and variance of this PDF can be easily found as

E [U] = $n\sigma^2$ and $\sigma_U{}^2 = 2n\sigma^4$ respectively.

If we let m=n/2, a positive integer, then the probability distribution function is given by [20, pp. 829].

$$p_U(u) = \frac{1}{\Gamma(m)\left(\frac{\overline{U}}{m}\right)^m} u^{m-1} \exp\left\{-\frac{u}{\overline{U}/m}\right\} \qquad u \geq 0 \tag{4.25}$$

With

$\overline{U} = E[U] = 2m\sigma^2$.

On the other hand, Gamma distribution is given by following equation,

$$p_G(g) = \frac{1}{\Gamma(a)b^a} g^{a-1} \exp\left(\frac{-g}{b}\right) \qquad g \geq 0 \quad \text{a} > 0, \text{b} > 0 \tag{4.26}$$

Comparing (4.25) and (4.26), we can draw an important conclusion about the relationship between Gamma distribution and the central chi-square distribution that the gamma distribution is equivalent to the central chi-square with 2m degrees of freedom.

If a=m and b=$\frac{\Omega}{m}$ and the mean $\overline{U} = \overline{G} = E[G] = 2m\sigma^2 = \Omega$

Consequently, the Nakagami-m distribution can be written in the following form,

$$p_Z(z) = \frac{2}{\Gamma(m)(\frac{\Omega}{m})^m} z^{2m-1} \exp\{-\frac{z^2}{\Omega/m}\} \tag{4.27}$$

Which is exactly same as equation (4.20) with $\Omega = 2m\sigma^2$ and

$$E\left[(Z^2-\Omega)^2\right]=E\left[(G-\overline{G})^2\right]=2.(2m).\sigma^4$$

Characteristic function of equation of (4.26) is given by

$$\Psi_G(jv)=(1-jv\frac{\Omega}{m})^{-m} \tag{4.28}$$

Comparing equation (4.28) with (4.23),

We can deduce the following relationship,

$$\Psi_G(jv)=\{\Psi_U(jv)\}^{\frac{2m}{n}} \tag{4.29}$$

With 2m > n and n=1, 2…

Having investigated theoretical relationships, we can generate Nakagami fading signals as given below.

Suppose that the 2m/n is an integer value, then

Gamma random variable is a sum of statistically independent and identically distributed central chi-square distributions. This can be formulated by following equation

$$G=\sum_{j=1}^{\frac{2m}{n}}U_j \tag{4.30}$$

Where U is a follows chi-square distribution.

Now, the central chi-square distribution can be characterized by a mapping, $\aleph=x^2$ where x is the normal distribution with zero mean and given variance

This relationship takes the following form,

$$U=\sum_{i=1}^{n}x_i^2 \tag{4.31}$$

Combining equations (4.30) and (4.31)

$$G = \sum_{j=1}^{\frac{2m}{n}} \sum_{i=1}^{n} x_i^2$$

$$G = \sum_{k=1}^{2m} x_k^2 \tag{4.32}$$

Thus we have established the relationship between a set of Gamma random variables and Normal random variables, which only demands '2m' to be an integer value.

Furthermore, Nakagami random process Z, can be obtained from Gamma random process G by a mapping

$$G = Z^2$$

OR

$$Z = \sqrt{G}$$

Thus we have established the relationship between Nakagami and Gamma distributions. Next we will see realization of actual Nakagami random process.

4.3) Sum-of-Sinusoids based Nakagami-m Simulator

In this section, we will discuss how to design new Nakagami-m simulator [14] using above relationships and existing Rayleigh fading models.

We can write equation (4.32) as

$$G = \alpha \sum_{k=1}^{P} X_k^2 + \beta X^2{}_{p+1} \tag{4.33}$$

With $P = \lfloor 2m \rfloor$ as an integer part. If m is real, the correlated remainder term $X^2{}_{p+1}$ is added to improve the accuracy of the Nakagami simulator.

The weights α and β play an important role in adapting integer and fractional part to achieve better efficiency.

We can infer from the equation (4.33)

Referring to the details of equations in [2], we can write

$$\aleph^2(2m) \overset{d}{=} \alpha \sum_{k=1}^{P} \aleph_k^2(1) + \beta \aleph^2{}_{p+1}(1) \tag{4.34}$$

$\overset{d}{=}$ Indicates that both left hand side and right hand side have same distribution.

Taking the first moments of equation (4.34) and noting the fact that $E\left[\aleph^2(m)\right] = m$ and $\text{var}\left[\aleph^2(m)\right] = 2m$, we get

$$P\alpha + \beta = 2m$$

$$P\alpha^2 + \beta^2 = 2m$$

Solving these two equations, we obtain

$$\alpha = \frac{2Pm \pm \sqrt{2Pm(P+1-2m)}}{P(P+1)} \tag{4.35}$$

$$\beta = 2m - \alpha P \tag{4.36}$$

Therefore the architecture of Nakagami-m simulator is given by

$$G(t) = \alpha \sum_{k=1}^{P} X_k^2(t) + \beta X_{P+1}^2(t) \tag{4.37}$$

Where X is a Gaussian process. Using equations, (4.12) and (4.13) we get

$$G(t) = \alpha \sum_{k=1}^{P} Y_{c,k}^{\ 2}(t) + \beta Y_s^2(t) \tag{4.38}$$

Equation (4.38) represents Gamma process and resultant Nakagami-m random process is given by

$$Z(t) = \sqrt{G(t)} = \sqrt{\alpha \sum_{k=1}^{P} Y_{c,k}^{\ 2}(t) + \beta Y_s^2(t)} \tag{4.39}$$

The equation (4.39) represents new sum-of-sinusoids based Nakagami-m simulator.4.

4.3.1) Higher Order Statistics

4.3.1.1) Squared Autocorrelation function

The squared envelope autocorrelation function is given by following equation

$$R_{g_z^2}(t_1, t_2) = E\left[G(t_1), G(t_2)\right] \tag{4.40}$$

Since $G = Z^2$, squared autocorrelation of Nakagami sequence is nothing but the autocorrelation of gamma sequence.

Therefore, we can write

$$\begin{aligned} R_{g_z^2}(t_1, t_2) = {} & p\alpha^2 E\left[Y_{c,i}^2(t_1), Y_{c,j}^2(t_2)\right]_{i=j} + \beta^2 E\left[Y_s^2(t_1), Y_s^2(t_2)\right] + p(p-1)\alpha^2 E\left[Y_{c,i}^2(t_1), Y_{c,j}^2(t_2)\right]_{i \neq j} + \\ & p\alpha\beta E\left[Y_{c,k}^2(t_1), Y_s^2(t_2)\right] + p\alpha\beta E\left[Y_s^2(t_1), Y_{c,k}^2(t_2)\right] \end{aligned} \tag{4.41}$$

Referring to [14], we can write squared autocorrelation of Nakagami sequence as

$$\begin{aligned} R_{g_z^2}(t_1, t_2) = {} & m^2 + mJ_0^2(w_m\tau) + mJ_4^2(w_m\tau) + (P\alpha^2 - \beta^2)J_0(w_m\tau)J_4(w_m\tau) + \\ & 4P\alpha\beta\left[\frac{2}{\pi}\int_0^{\frac{\pi}{2}} \sin(4\alpha)\cos(w_m\tau\cos\alpha)d\alpha\right]^2 \end{aligned} \tag{4.42}$$

The equation (4.42) represents Nakagami-m squared envelope autocorrelation associated with (4.39).

4.3.1.2) Level Crossing Rate (LCR)

The Level crossing rate at which envelope crosses a given level R as discussed in previous section is given by

$$N_R = \int_0^{\infty} R' p(R', r = R) dR'$$

Referring to Appendix A. 1 for detailed derivation of level crossing rate, and is given by

$$N_R = \sqrt{2\pi} f_m \frac{m^{m-0.5}}{\Gamma(m)} r^{2m-1} \exp(-mr^2) \tag{4.40}$$

This is an exact and closed form expression for the level crossing rate of the Nakagami-m fading signal.

4.3.1.3) Average Fade Duration (AFD)

The average duration of fades T_R below r=R is given by

$$T_R = \frac{p(r \le R)}{N_R} = \frac{1}{N_R} \int_0^R p(r) dr$$

Referring to the derivation in Appendix A. 2, we can formulate the result as below

$$T_R = \frac{2\sqrt{m}\left[\psi(m, \rho)\right]}{\sqrt{2\pi} f_d \rho^{(2m-1)} \exp(-m\rho^2)} \tag{4.41}$$

Where $\psi(a,b) = \int_0^b z^{2a-1} \exp(-az^2) dz$

CHAPTER 5

GENERATION OF CORRELATED NAKAGAMI-m FADING CHANNEL: A DECOMPOSITION TECHNIQUE

In the previous chapter we have seen the sum of sinusoids method to generate Nakagami-m fading samples. It is fairly simple method to generate samples from Gaussian processes, which itself can be easily generated. In this chapter we will use Direct Sum Decomposition method to generate multi-branch Nakagami channel with given covariance matrix and fading parameter.

5.1) Introduction

A different approach should be adopted to generate correlated Nakagami vector with an arbitrary covariance matrix. We know that Nakagami variable is a square root of Gamma variable. A decomposition principle introduces a gamma vector as set of independent vectors, which in turn can be produced from a set of correlated Gaussian processes such as given in previous chapters. The reference [2] provides details of decomposition technique. Only key points pertaining to sum of sinusoids method are presented in this chapter.

5.2) Relationship between covariance matrices of different distributions

Our aim is to generate n –by-1 correlated Nakagami vector Z with fading parameter m and covariance matrix R_z. [2]

We define,

$x \sim N(0, R_x)$ $\quad$ $y \sim GM(m, R_y)$ $\quad$ $z \sim NK(m, R_z)$ Indicate that x, y, z follow joint Gaussian, Gamma and Nakagami distribution.

As shown before, there are no direct methods to generate Nakagami sequence in literature; direct sum decomposition method will be used.

The approach here used is

$X_k \text{ ---------} > Y \text{ ----------} > Z$

Where X_k is a set of independent Gaussian vectors. Gaussian vectors are easy to generate and Nakagami vector can be obtained by taking square root of gamma vector, which is denoted as

$$Z = Y^{(1/2)} \tag{5.1}$$

The characteristic function of gamma vector is given by

$$\phi_y(s) = \det(I - SA)^{-m} \tag{5.2}$$

Where S is a diagonal matrix of the variables in the transform domain. The positive-definite matrix A is determined by the covariance matrix structure of y, and is given by

$$A(k,l) = \sqrt{\frac{R_y(k,l)}{m}} \qquad \text{I.e.} \qquad R_y = mA^2 \tag{5.3}$$

Given R_z, we need systematic approach to determine R_y, R_x.

5.2.1) Determination of R_y from R_z

In typical problem like this we have been given cross-coefficient matrix of end process. I.e. Nakagami process. We will first establish the relation between variance of Gamma and Nakagami Vectors and Relation between cross-correlation coefficient matrices of both the processes.

The resultant covariance matrix for gamma RV will is given by

$$R_y(i,j) = v(i,j)\sqrt{\text{var}(y_i)\,\text{var}(y_j)} \tag{5.4}$$

5.2.1.1) Relationship between variances of Gamma and Nakagami RV

Suppose that we want to determine the variance of gamma process y in terms of variance of Nakagami Process z.

$$\text{var}[y] = \frac{\text{var}^2[z]}{m}\left[1 - \frac{1}{m}\frac{\Gamma^2(m+\frac{1}{2})}{\Gamma^2(m)}\right]^{-2} \tag{5.5}$$

5.2.1.2) Cross-correlation

Given covariance structure of Nakagami sequence, the cross-correlation coefficient matrix can be calculated as

$$\rho_{i,j} = \frac{R_z(i,j)}{\sqrt{R_z(i,i)R_z(j,j)}} \tag{5.6}$$

Using equation (5.5), the cross-correlation coefficient matrix $v(i,j)$ of gamma vector can be calculated from the recursive algorithm in [2].

Having calculated the correlation matrix v (i, j) and variance from equation (5.4), the covariance matrix is given by equation (5.3).

In the next section, we will see direct sum decomposition to generate Nakagami n by 1 fading sequence.

5.3) Direct Sum Decomposition

From statistical theory we know that gamma vector can be represented in terms of a set of Gaussian vectors as given below

$$U = X^2$$

The characteristic function of Gamma vector U is given by

$$\phi_u(S) = E\left[\exp(ju_1t_1 + ju_2t_2 + ... + ju_nt_n)\right]$$

$$\phi_u(S) = \int_{-\infty}^{\infty} (2\pi)^{-0.5n} \det(R_x)^{-0.5} \exp(-0.5x^T R_x^{-1} x + x^T Sx)dx \tag{5.7}$$

$$\phi_u(S) = \det(I - 2SR_x)^{-0.5}$$

Observing that equation (5.2) and (5.7) has similar forms, we can write equation (5.2) as

$$\phi_u(S) = \prod_{k=1}^{2m} \det(I - 2SR_x)^{-0.5} \tag{5.8}$$

$$R_y = m(2R_x)^2 = 4mR_x$$

Solving above equation, we get the covariance matrix of Gaussian vectors as below

$$R_x = \frac{1}{2\sqrt{m}} R_y^{1/2} \tag{5.9}$$

The probability density function of independent variables is Fourier transformed to the product in characteristic function domain. When transformed back to the original domain,

left hand side of equation (5.8) is simply equal gamma random vector i.e. Y whereas right hand side yields a sum of U. This can be written in the following form

$$Y = \sum_{k=}^{2m} U_K = \sum_{k=1}^{2m} X_k^2 \tag{5.10}$$

This expression assures that the Nakagami vector has the same direct-sum decomposition as that of its scalar counterpart and the correlation is uniquely determined by the correlation of Gaussian vectors.

Therefore Nakagami sequence is given by

$$Z = Y^{(1/2)}$$

$$Z = \left(\sum_{k=1}^{2m} U_k \right)^{(1/2)}$$

From equation (5.10) we can write

$$Z = \left[\sum_{k=1}^{2m} X_k^2 \right]^{(1/2)} \tag{5.11}$$

This expression allows us to obtain correlated Nakagami vector from set of independent Gaussian vectors.

From Equation (5.5) and (5.9) we can write

$$\begin{aligned} R_x &= \varsigma \,\mathrm{var}[z(k)] && \mathrm{k} = 1 \\ &= \varsigma \{ \mathrm{var}[z(k)] \;\; \mathrm{var}[z(l)] \;\; \mathrm{v(k,l)} \}^{1/2} && \mathrm{k} \neq 1 \end{aligned} \tag{5.12}$$

Where

$$\varsigma = \frac{1}{2m} \left[1 - \frac{1}{m} \frac{\Gamma^2(m + 0.5)}{\Gamma^2(m)} \right]^{-1} \tag{5.13}$$

If size of x is not very large (for diversity application), we can generate samples of independent Gaussian random variables from covariance matrix R_x found above.

We can use the technique of Cholskey Decomposition to decompose R_x such that

$$R_x = LL' \tag{5.14}$$

Where ‘denotes Hermition transpose and L is lower triangular matrix obtained after decomposition

Next step is to generate independent and identically distributed Gaussian sequence with zero mean and unit variance. This can be generated using rand function in Matlab or any Gaussian random process given in chapter 4

$$E_k \approx N(0,I) \tag{5.15}$$

Therefore we can write correlated Gaussian vector in terms of i.i.d. Gaussian vectors as

$$X_k = L * E_k \tag{5.16}$$

This is a simple method to generate correlated Nakagami fading channel for diversity application.

In previous section, it was assumed that m holds integer value. If ‘m’ is real, different approach is taken.

As discussed in previous chapter, integral part of ‘2m’ is given by

$$P = \lfloor 2m \rfloor$$

Therefore, Y can be written as

$$Y(t) = \alpha \sum_{k=1}^{P} X_k^2(t) + \beta X_{P+1}^2(t) \tag{5.17}$$

and corresponding correlated Nakagami vector channel for diversity applications is given by

$$Z(t) = \sqrt{Y(t)} = \sqrt{\alpha \sum_{k=1}^{P} X_k^2(t) + \beta X_{P+1}^2(t)} \tag{5.18}$$

When ‘m’ is real, β provides fine correction to the process. When ‘m’ is a multiple of ½, β is always zero. Therefore no correction is provided. This is exactly what we have seen earlier in section (5.3), Direct Sum Decomposition.

5.4) Algorithm

Given cross-correlation matrix $\rho(i,j)$ of end process i.e. Nakagami Process, variance vector $P_z = R_z(i,i)$ the following steps are taken to generate correlated Nakagami fading channel.

- Determine the cross-correlation of gamma RV using algorithm in [2 equations 20-23]
- Determine R_x using equations (5.12) and (5.13)
- Determine X_k using method of Cholskey Decomposition.
- Determine Gamma RV Y as

$$Y = \sum_{k=1}^{2m} X_k^2 \qquad 2\text{m} = \text{integer}$$

$$= \alpha \sum_{k=1}^{P} X_k^2 + \beta X_{P+1}^2 \qquad \text{otherwise}$$

- The Desired Nakagami vector Z is given by

$$Z = Y^{(1/2)}$$

CHAPTER 6

SIMULATION ANALYSIS AND DISCUSSIONS

This chapter is mainly divided into two sections

- Sum of Sinusoids
- Direct Sum decomposition for correlated Nakagami fading channel for diversity application.

6.1) Analysis of Sum-of-Sinusoids Technique

In order to realize sum-of-sinusoids, we used improved Jake's Model. However, other low-pass Gaussian processes given in section 4.1

Let's review original Jake's Model and improved model in short.

The Inphase and quadrature processes suggested by Jakes are given below

$$X_c(t) = \sqrt{\frac{4}{N}} \sum_{n=1}^{M+1} a_n \cos(w_n t)$$

$$X_s(t) = \sqrt{\frac{4}{N}} \sum_{n=1}^{M+1} b_n \cos(w_n t) \qquad (6.1.1)$$

Where different Parameters are given below

N=4M+2 and $w_d = 2\pi f_d$ is maximum Doppler frequency.

$$
\begin{aligned}
a_n &= 2\cos\beta_n && n = 1,2,3,...,M \\
&= \sqrt{2}\cos\beta_{M+1} && n = M+1
\end{aligned}
$$

$$
\begin{aligned}
b_n &= 2\sin\beta_n && n = 1,2,3,...,M \\
&= \sqrt{2}\sin\beta_{M+1} && n = M+1
\end{aligned}
$$

(6.1.2)

$$
\begin{aligned}
w_n &= \frac{\pi n}{M} && n = 1,2,3,...,M \\
&= \frac{\pi}{4} && n = M+1
\end{aligned}
$$

$$
\begin{aligned}
\beta_n &= w_d \cos\left(\frac{2\pi n}{N}\right) && n = 1,2,3,...,M \\
&= w_d && n = M+1
\end{aligned}
$$

It was shown that the signal produced by above model is not Wide sense Stationery [21] as autocorrelation not only depends upon time difference but also on time advancement. One more drawback is that inphase and quadrature components share same frequency values.

The improvement suggested is to add random phases to low frequency oscillators. By adding random variables we are able to reduce correlation between the two processes. The inphase and quadrature processes of the new model are given below

$$
\begin{aligned}
X_c(t) &= \sqrt{\frac{4}{N}} \sum_{n=1}^{M+1} a_n \cos(w_n t + \psi_n) \\
X_s(t) &= \sqrt{\frac{4}{N}} \sum_{n=1}^{M+1} b_n \cos(w_n t + \psi_n)
\end{aligned}
$$

(6.1.3)

Where ψ_n is a uniformly distributed over interval $[-\pi, \pi]$.

Using equation (4.39), we can write

$$Z(t) = \sqrt{G(t)} = \sqrt{\alpha \sum_{k=1}^{P} X_{c,k}^{2}(t) + \beta X_{s}^{2}(t)} \qquad (6.1.4)$$

The figures (6.1.1) and (6.1.2) show graphical representation of equations (6.1.2) and (6.1.4)

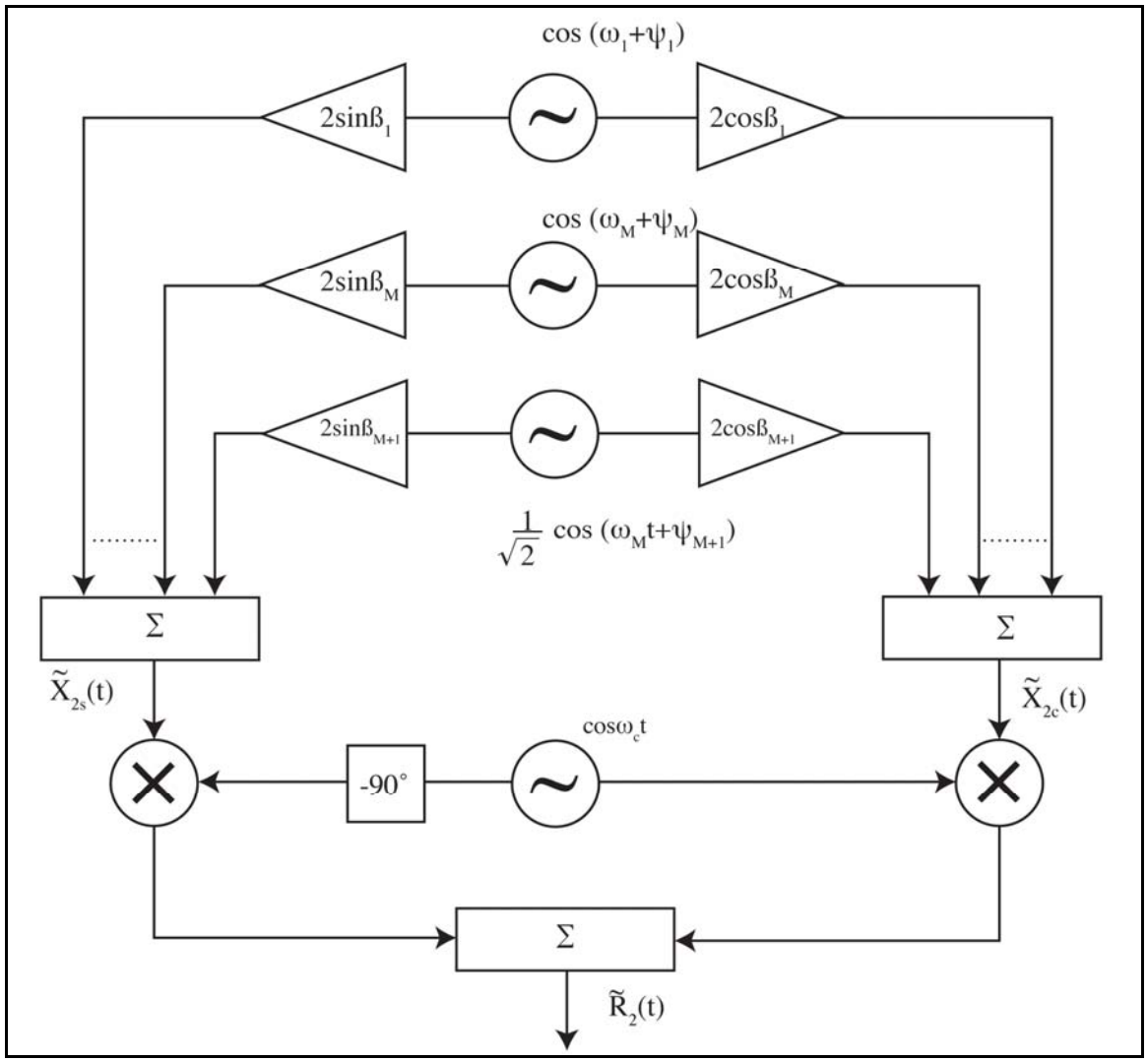

Figure 6.1.1: Improved Jake's Model

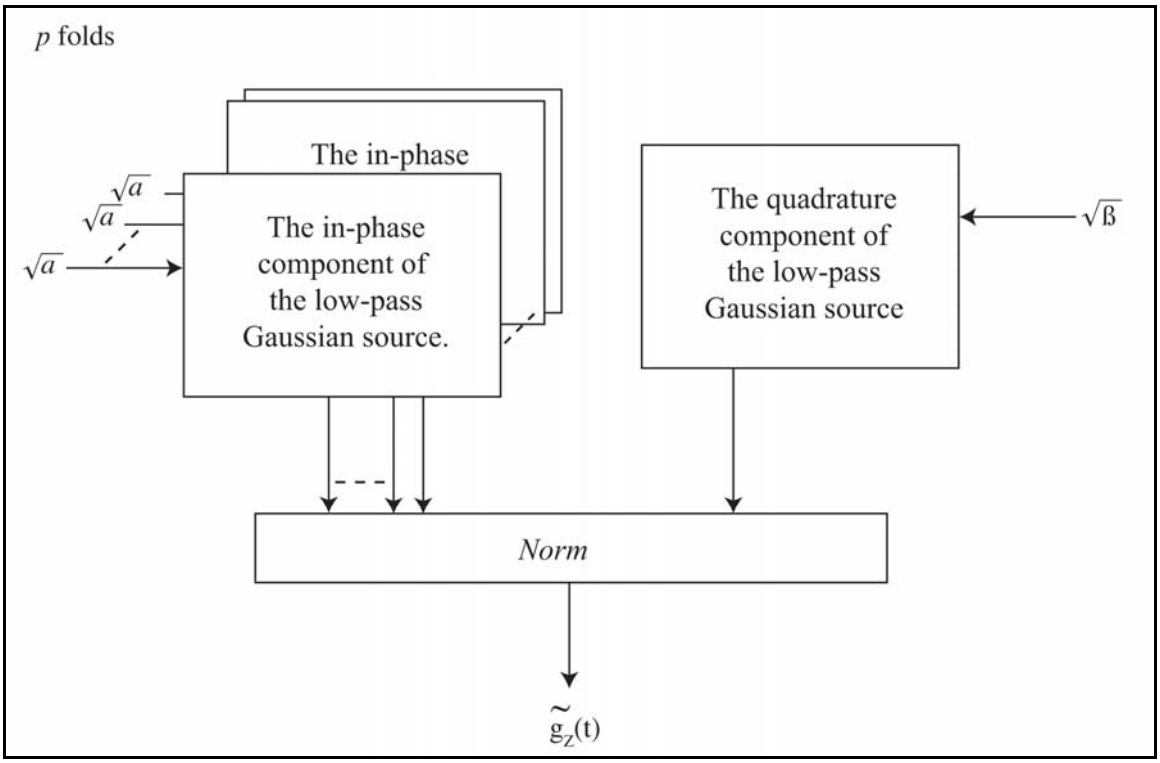

Figure 6.1.2: Nakagami Simulator Architecture.

This is the realization of sum-of-sinusoids method for Nakagami-m fading channels. We have used the following data.

N=No. Of Samples-50000; f_d =Maximum Doppler Frequency=100 Hz; Ts=Sampling Period =0.00025 sec. The ensemble average of autocorrelation is carried out over 25 iterations in order to get better estimate.

6.1.1) Simulated and Theoretical PDF, Autocorrelation, Received field Intensity, Level Crossing Rate and Average Fade Duration for different values of m

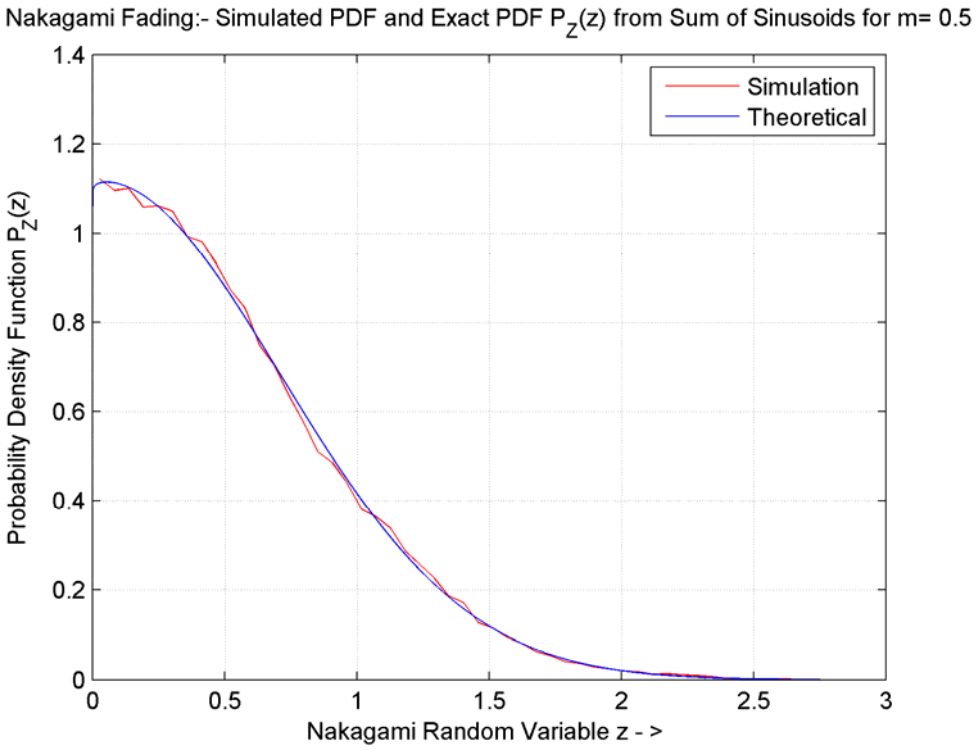

Figure 6.1.3: Simulated and Theoretical PDF for m=0.5

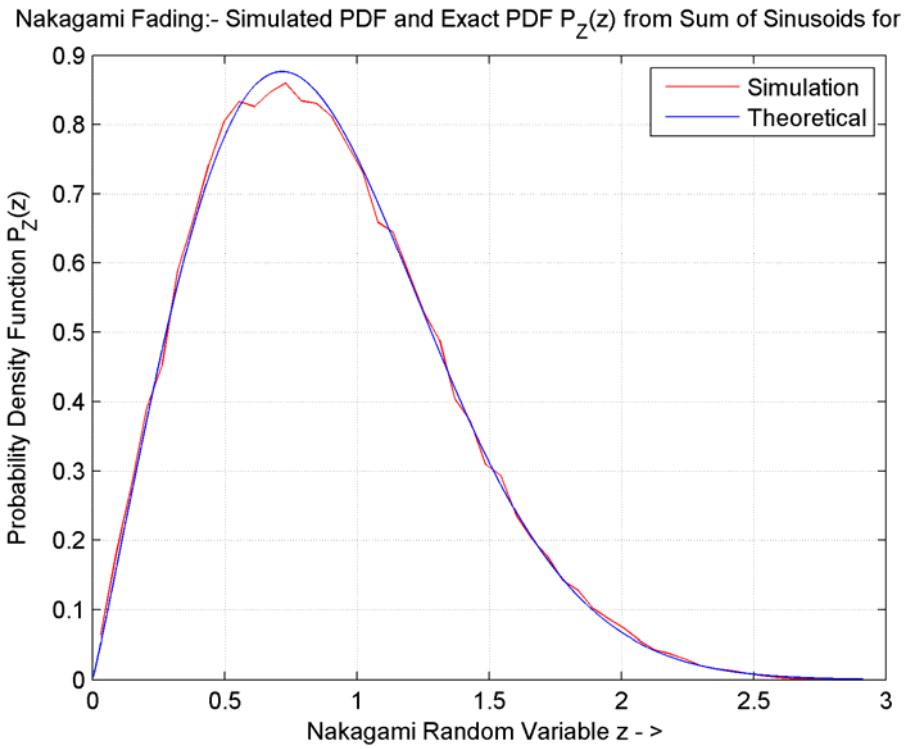

Figure 6.1.4: Simulated and Theoretical PDF for m=1

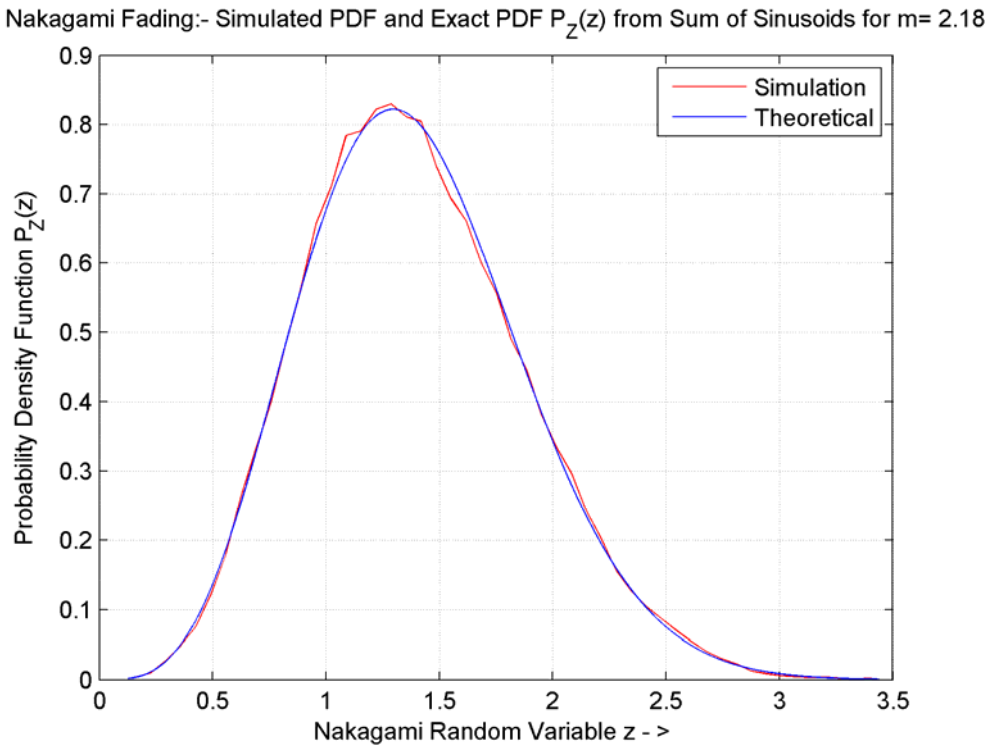

Figure 6.1.5: Simulated and Theoretical PDF for m=2.18

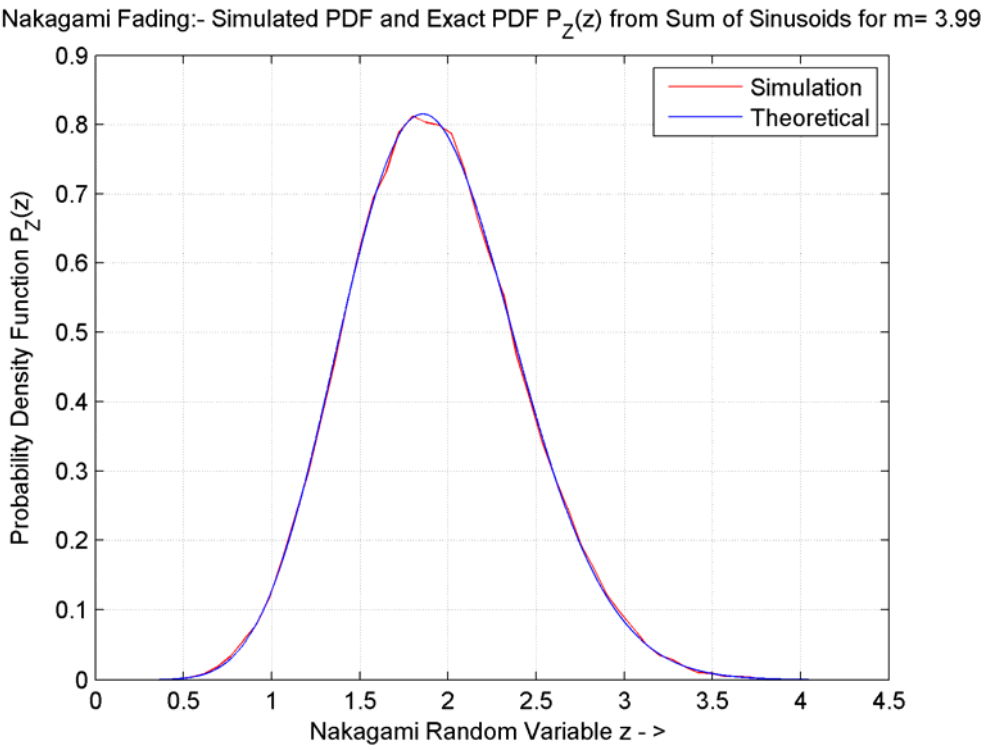

Figure 6.1.6: Simulated and Theoretical PDF for m=3.99

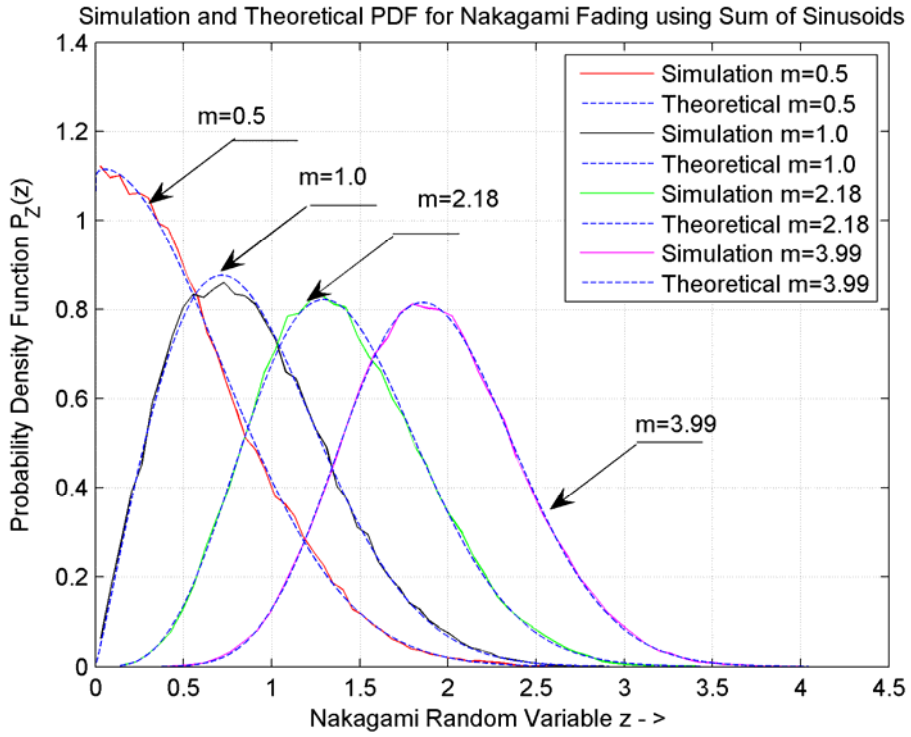

Figure 6.1.7: Composite Simulated and Theoretical PDF

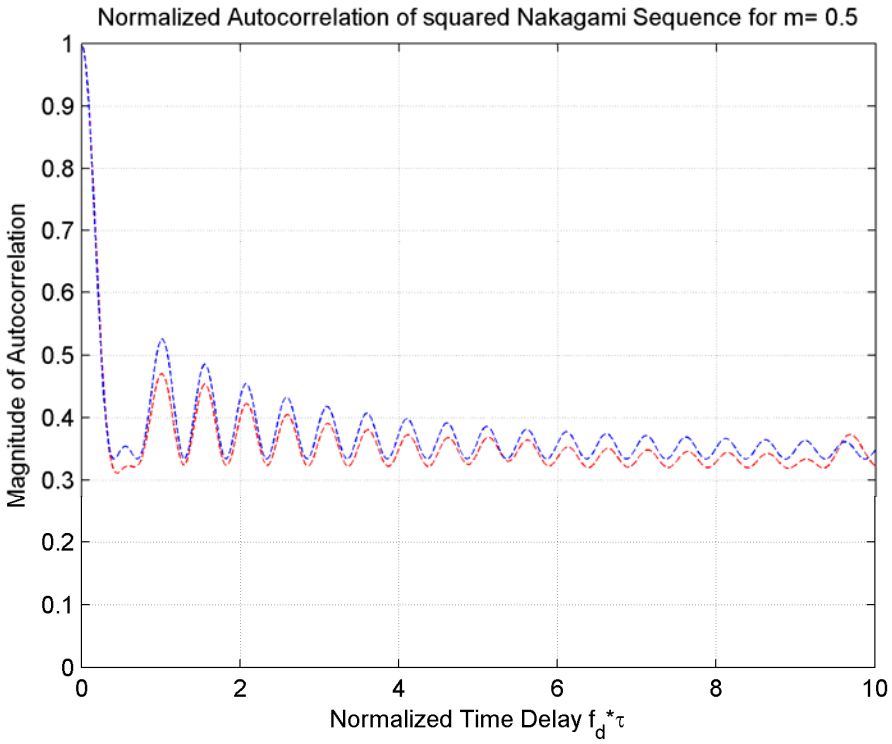

Figure 6.1.8: Normalized Simulated and Theoretical Autocorrelation for m=0.5

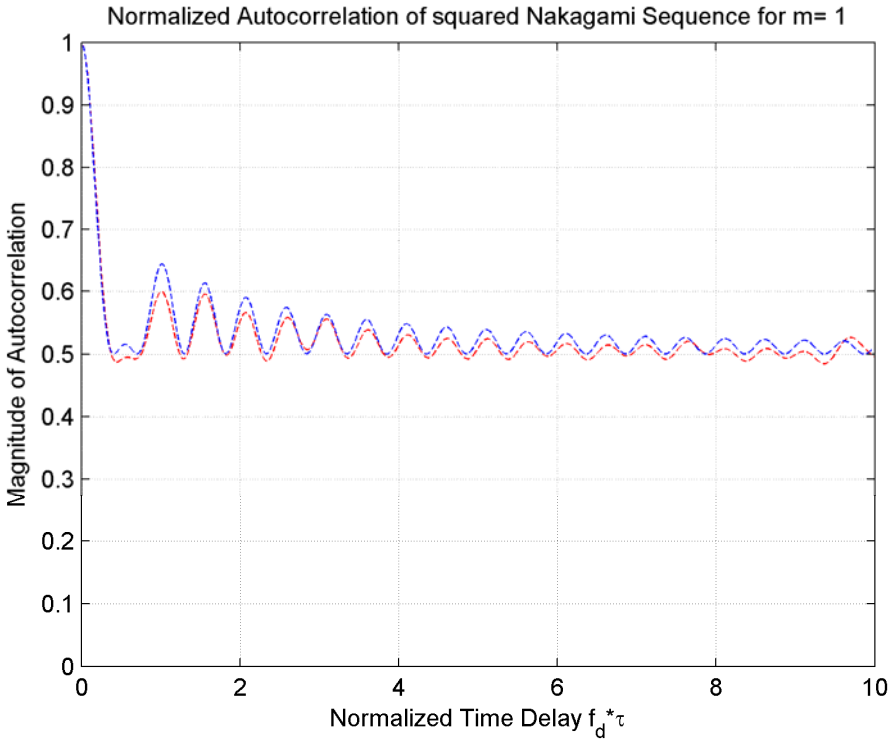

Figure 6.1.9: Normalized Simulated and Theoretical Autocorrelation for m=1

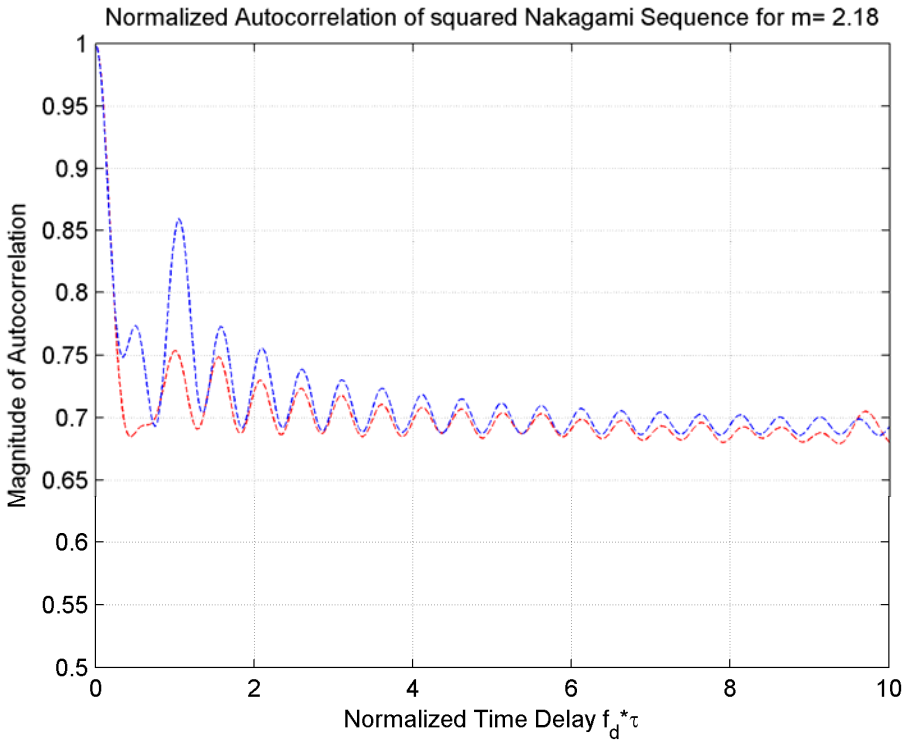

Figure 6.1.10: Normalized Simulated and Theoretical Autocorrelation for m=2.18

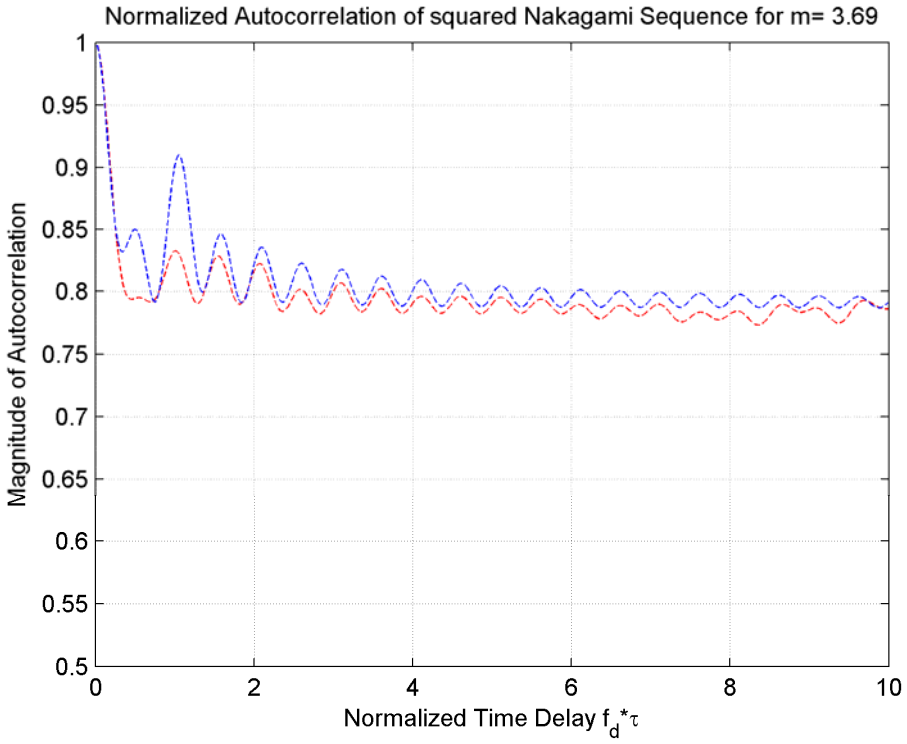

Figure 6.1.11: Normalized Simulated and Theoretical Autocorrelation for m=3.69

The ensemble normalized autocorrelation and reference autocorrelation plots are above. The received field intensity in dB scale is shown below.

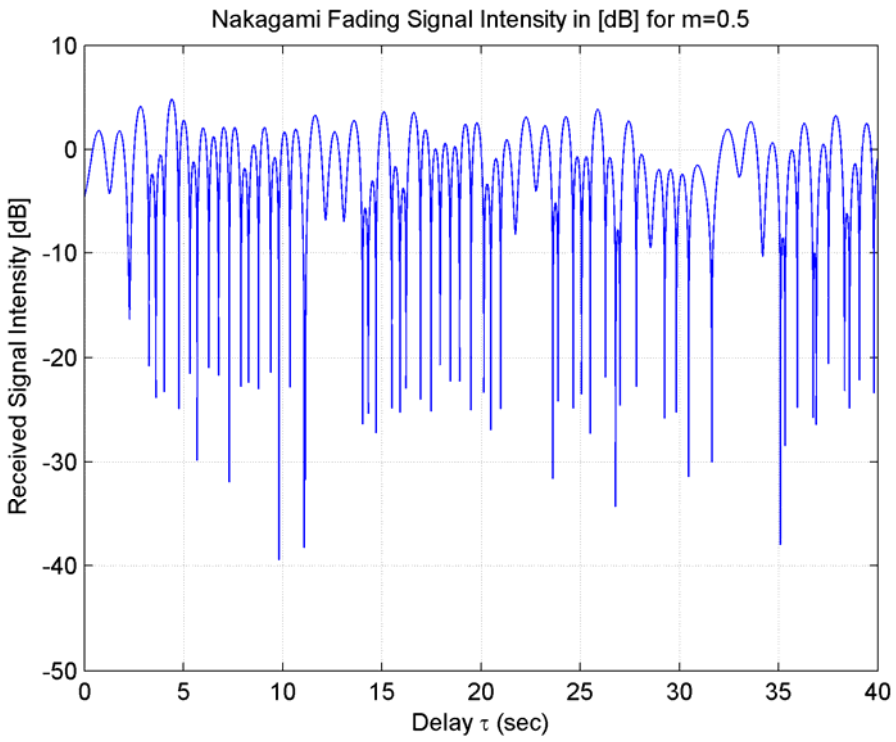

Figure 6.1.12: Received Field Intensity in dB for m=0.5

As we can see that fades around 40 dB or more can be seen for m=0.5 which is the worst case of fading in Nakagami environment. The intensity of fading decreases as 'm' increases.

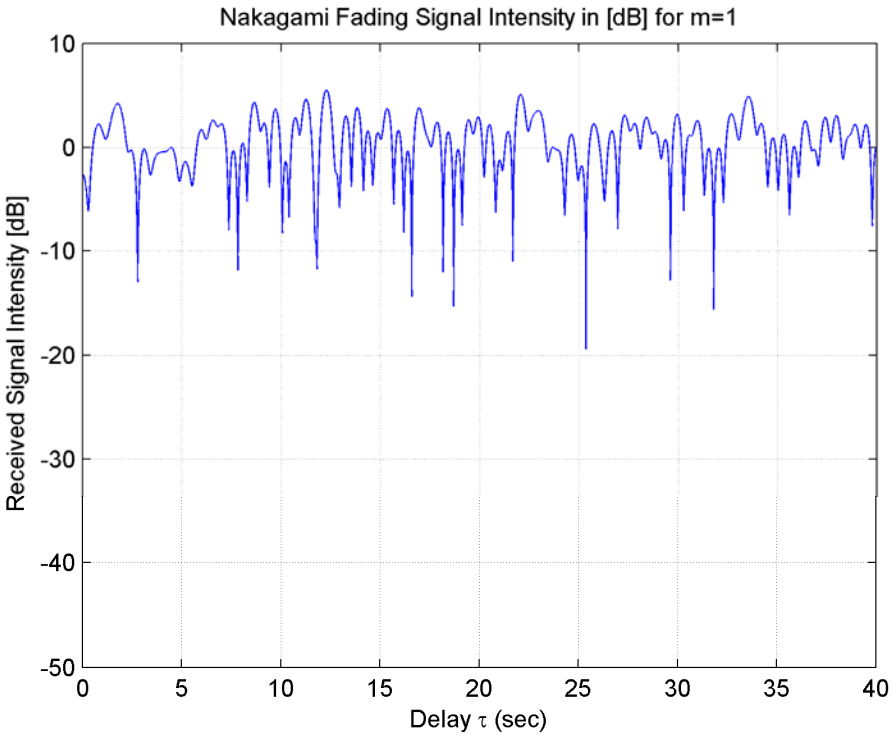

Figure 6.1.13: Received Field Intensity in dB for m=1

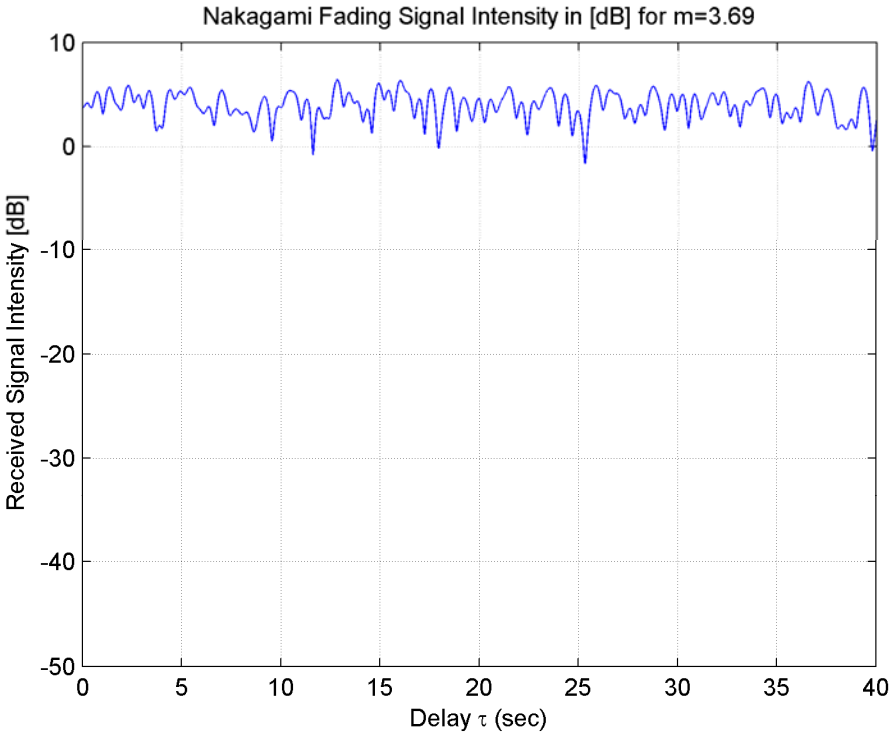

Figure 6.1.14: Received Field Intensity in dB for m=3.69

Level crossing rate and Average fade Duration are another important second order statistics of any simulator.

LCR and AFD for sum-of-sinusoids based simulator are given by equations (4.40) and (4.41)

Level Crossing Rate:-

Theoretical Equation: - $N_R = \sqrt{2\pi} f_m \frac{m^{m-0.5}}{\Gamma(m)} r^{2m-1} \exp(-mr^2)$

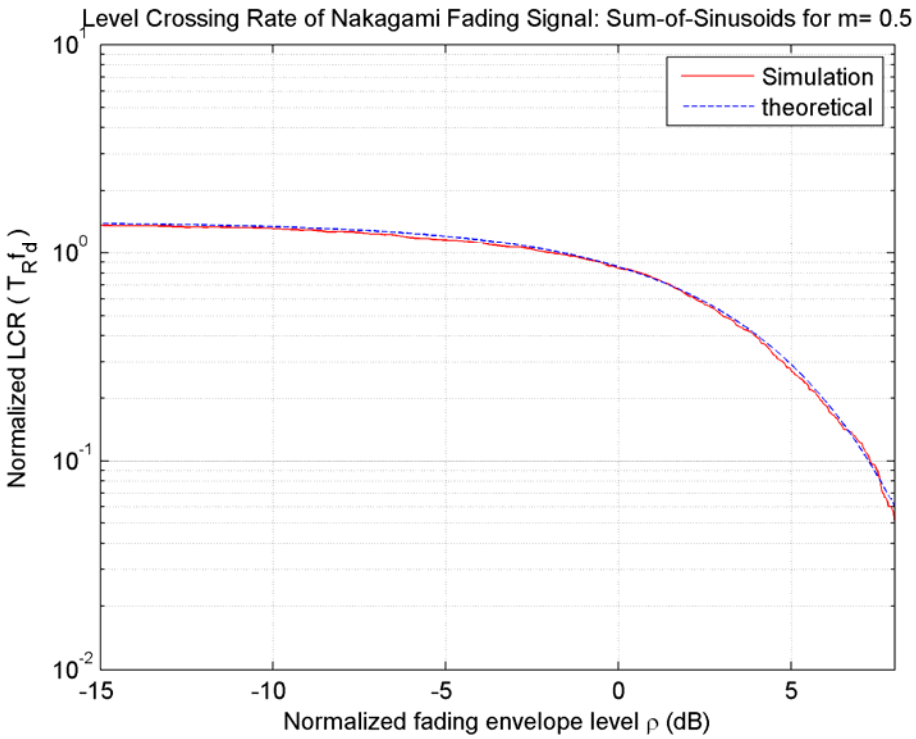

Figure 6.1.15: Level Crossing Rate in log-scale for m=0.5

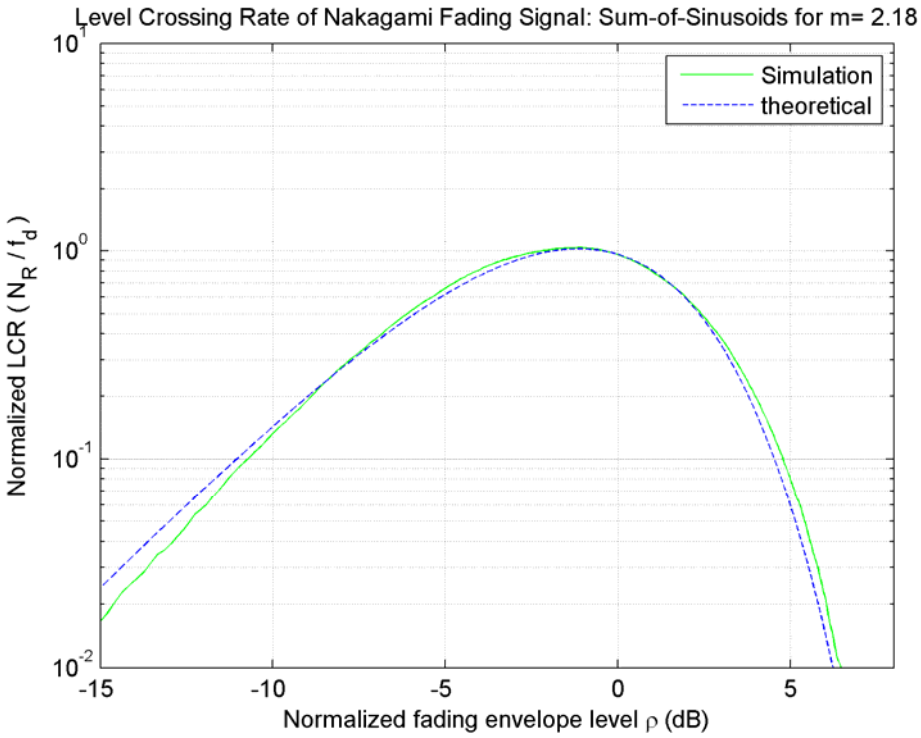

Figure 6.1.16: Level Crossing Rate in log-scale for m=2.18

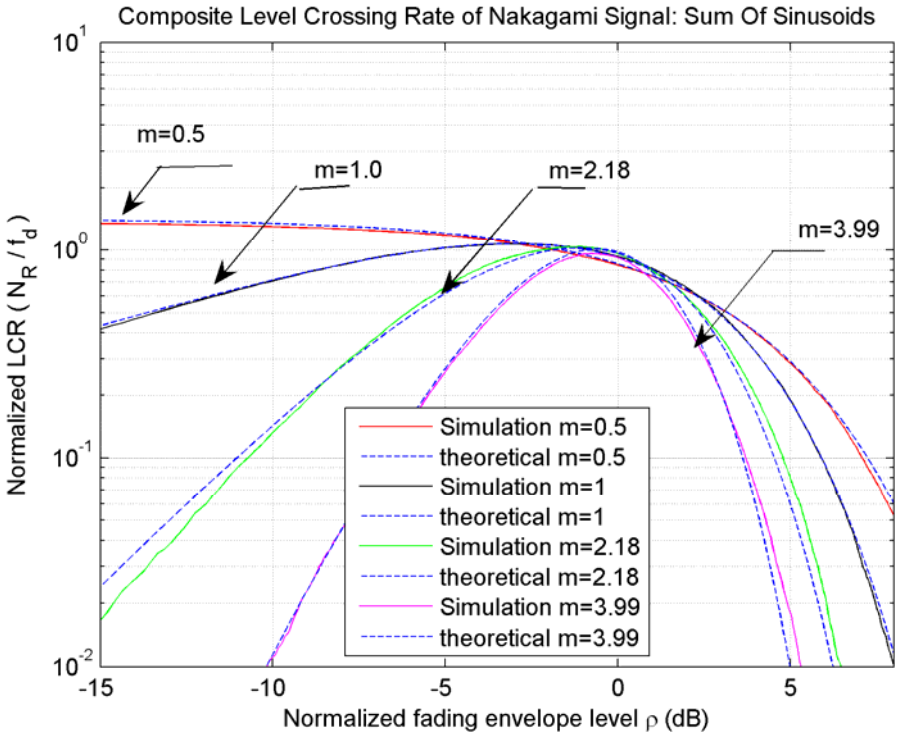

Figure 6.1.17: Composite Level Crossing Rate in log-scale

Average Fade Duration: - T_R

Theoretical Equation: -

$$T_R = \frac{2\sqrt{m}\left[\psi(m,\rho)\right]}{\sqrt{2\pi}\, f_d \rho^{(2m-1)} \exp(-m\rho^2)}$$

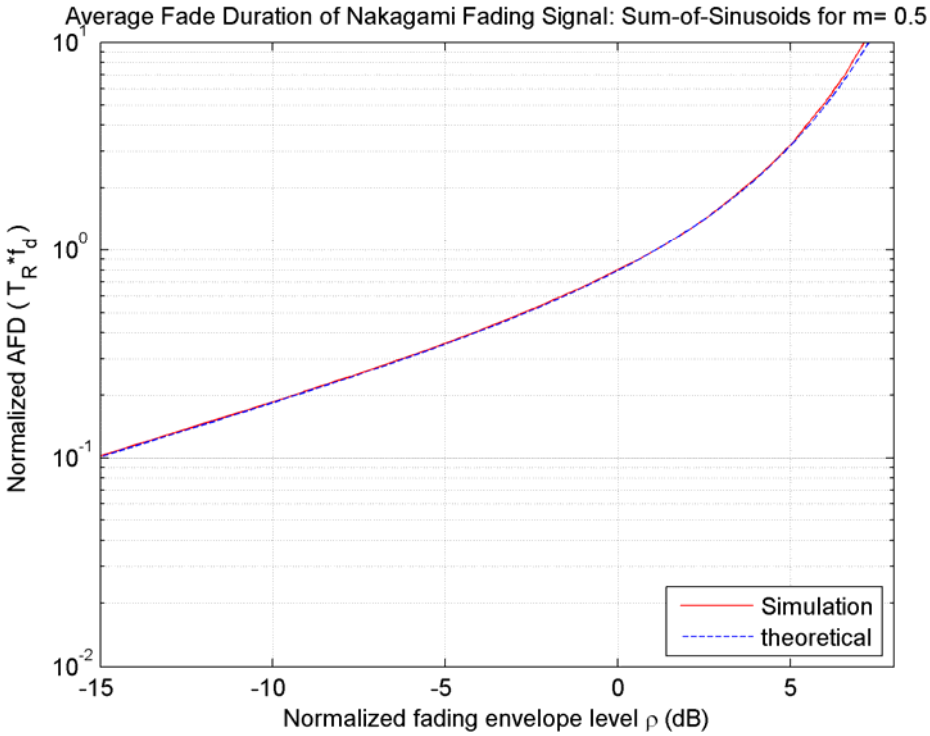

Figure 6.1.18: Average Fade Duration in log-scale for m=0.5

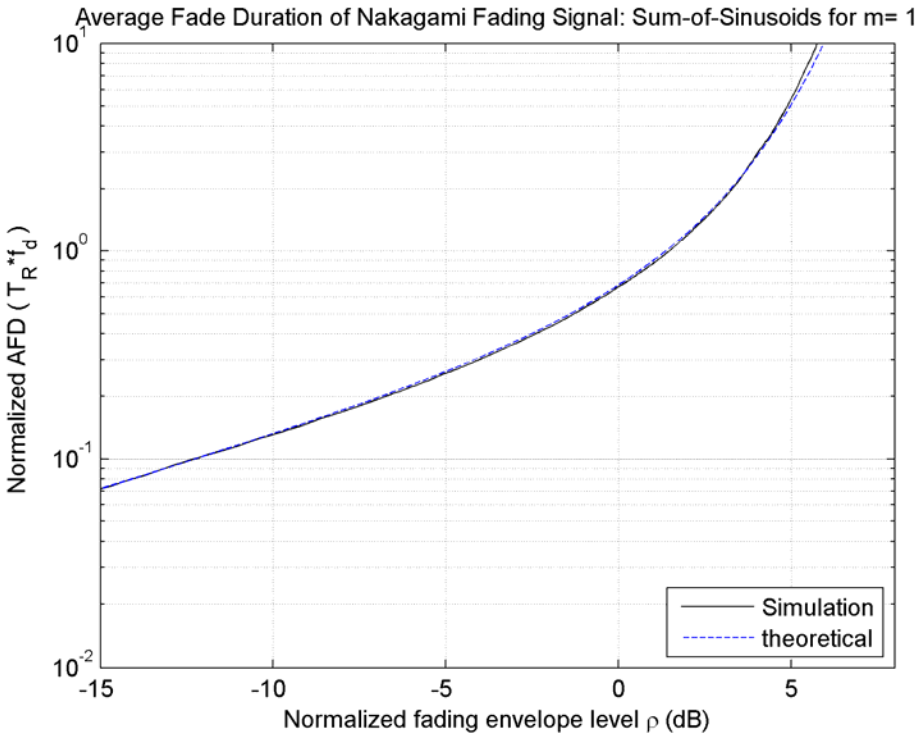

Figure 6.1.19: Average Fade Duration in log-scale for m=1.0

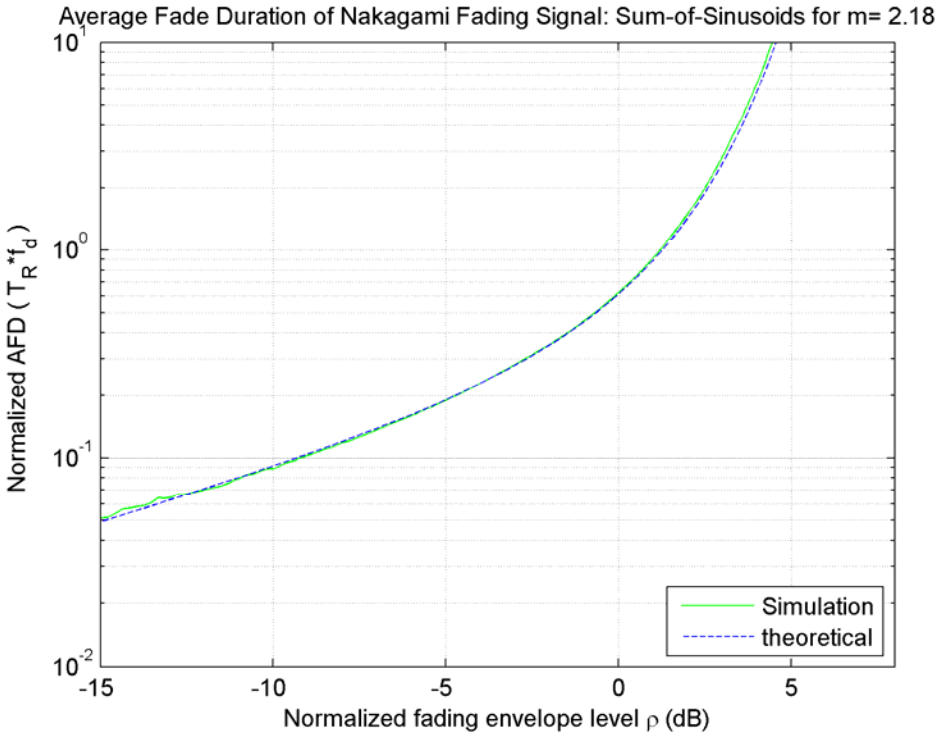

Figure 6.1.20: Average Fade Duration in lo-scale for m=2.18

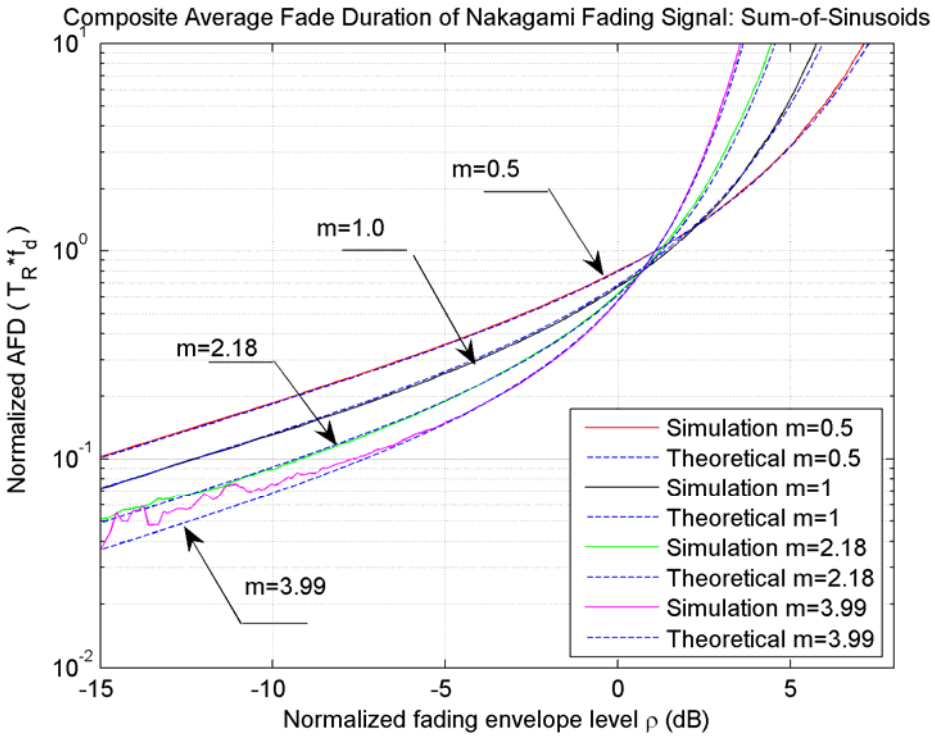

Figure 6.1.21: Average Fade Duration in lo-scale for m=1.0

6.1.2) Discussions

- The plots above show that the simulated data matches closely with theoretical probability density functions.
- For m=0.5, simulated data follows half-Gaussian distribution, m=1 it follows Rayleigh distribution which is consistent with the features of Nakagami distribution pointed out in section 2.4.3. For higher values of m, e.g. m=3.99, it exhibits Gaussian distribution.
- The sample autocorrelation function shows very close agreement with theoretical autocorrelation function implemented by equation (4.42).

- As the value of m increases, autocorrelation function approaches unity, which can be easily seen, from the graph.
- It has been verified that probability density functions match with theoretical ones given by other low-pass Gaussian processes.
- The received signal intensity in dB plots shows that m=0.5 is severe case of fading. As m increases, the severity of fading decreases leading to no fading condition for $m = \infty$
- Although the probability density functions match well, there will be some errors due to the mismatch of first two moments of the distribution.
- We also studied important second order characteristics. I.e. Level crossing rate and Average fade duration. The plots for both show excellent agreement with theoretical results.

6.2) Analysis of Decomposition Technique

In this section, analysis has been carried out for arbitrary covariance matrix and m=2.18 and 2.5

Our aim is to generate multi-branch data, which follows a joint Nakagami fading with the cross-correlation data obtained which matches closely with [21]

$$\rho_z = \begin{bmatrix} 1.000 & 0.795 & 0.604 & 0.372 \\ 0.795 & 1.000 & 0.795 & 0.604 \\ 0.604 & 0.795 & 1.000 & 0.795 \\ 0.372 & 0.604 & 0.795 & 1.000 \end{bmatrix}$$

With variance vector $P_z = [\ 2.16 \quad 1.59 \quad 3.32 \quad 2.78\ ]$ (6.2.1)

Next step is to calculate correlation matrix of corresponding Gamma vectors.

There are two possible ways to obtain it.

When all the diversity branches have same m-parameter, the relationship between gamma correlation coefficient ρ_y and the corresponding Nakagami correlation coefficient is given by the expression (139) in [1],

For n=1, we get

$$\rho_z = \frac{\Gamma^2(m+0.5)}{\Gamma(m)\Gamma(m+1) - \Gamma^2(m+0.5) \times [{}_2F_1(-0.5,-0.5;m,\rho_y) - 1]}$$

Where ${}_2F_1(*)$ is the hypergeometric function.

Numerically, ρ_z and ρ_y are equal. Therefore we can either directly equate ρ_y with ρ_z which is shown by the graph below or we can calculate using an algorithm mentioned in section [5.4]

The figure shows the value of ρ_z, vs. ρ_y as computed from above equation for m=1, 5 and 10.It clearly shows that ρ_y is almost identical to ρ_z.

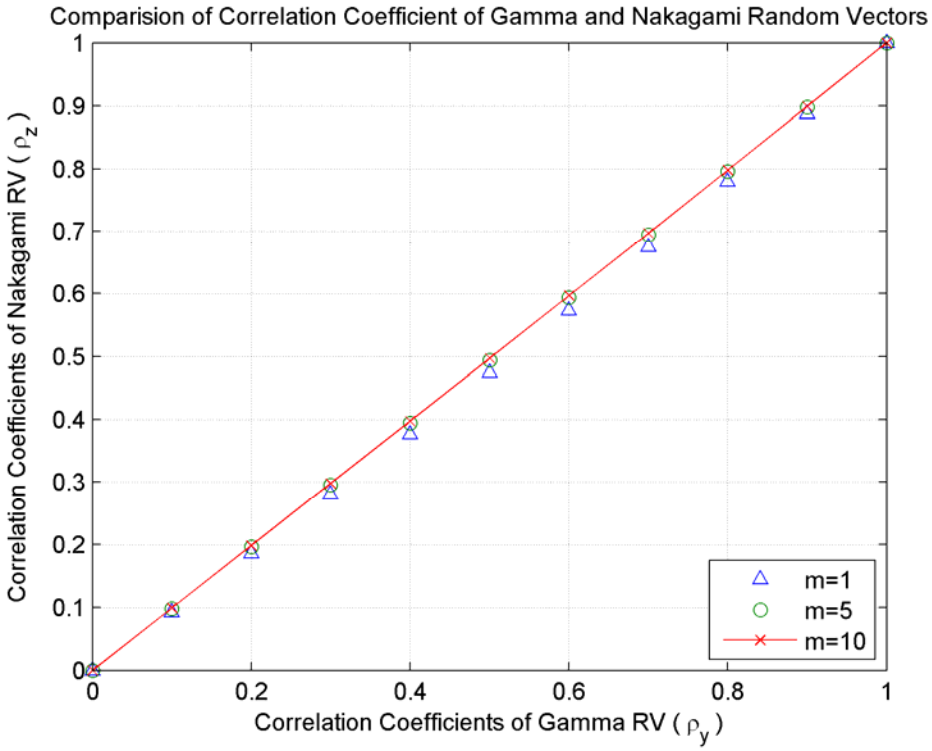

Figure 6.2.1 Graphical Comparison of Gamma and Nakagami Cross-Correlation Coefficients.

Setting margin for relative error to be up to 4 digits, Algorithm converges in few steps.

We get correlation vector for gamma RV as

v= [1.0000 0.8078 0.6197 0.3874] (6.2.2)

Next step is to calculate covariance matrix of correlated Gaussian Random vector from equations (5.12) and (5.13).

The value of ς found out to be ς**=2.1366** (6.2.3)

Now using equations (5.12), (6.2.1), and (6.2.2) and (6.2.3) we get,

$$R_x = \begin{matrix} \mathbf{4.6085} & \mathbf{3.5538} & \mathbf{4.4976} & \mathbf{3.2542} \\ \mathbf{3.5538} & \mathbf{3.3924} & \mathbf{4.4059} & \mathbf{3.5311} \\ \mathbf{4.4976} & \mathbf{4.4059} & \mathbf{7.0834} & \mathbf{5.8258} \\ \mathbf{3.2542} & \mathbf{3.5311} & \mathbf{5.8258} & \mathbf{5.9313} \end{matrix}$$

Now, we use Cholskey decomposition method to decompose R_x to get Lower Triangular matrix L.

Using L above and m=2.18, using equations (4.35) and (4.36),

We get $\alpha = 1.0390$ and $\beta = 0.2038$

Independent and identical Gaussian sequence can be generated using in-built ***rand*** function in MATLAB.

Thus we generate N =50000 samples for each diversity branch, using steps given in section (5.4), we generate fading samples for each diversity branch.

Estimated covariance matrix for Nakagami vector channel found out to be

$$\tilde{R}_z = \begin{matrix} \mathbf{2.1380} & \mathbf{1.4613} & \mathbf{1.6079} & \mathbf{0.9109} \\ \mathbf{1.4613} & \mathbf{1.5912} & \mathbf{1.8145} & \mathbf{1.2604} \\ \mathbf{1.6079} & \mathbf{1.8145} & \mathbf{3.3338} & \mathbf{2.4009} \\ \mathbf{0.9109} & \mathbf{1.2604} & \mathbf{2.4009} & \mathbf{2.7681} \end{matrix}$$

Corresponding cross-correlation coefficients are

$\tilde{\rho}_z =$ **[1.0000 0.7985 0.6073 0.3762]**

And estimated variance vector is

$\tilde{P}_z =$ **[2.1380 1.5912 3.3328 2.7681]**

The following table summarizes the results and relative errors among different parameters.

Parameter	Theoretical Values	Practical Values	Error (%)
Cross-Correlation Coefficients $\tilde{\rho}_z$	[1 0.795 0.604 0.372]	[1 0.7985 0.6073 0.3762]	**0.43 0.543 1.12**
Variance Vector $\tilde{P}_z$	[2.16 1.59 3.32 2.78]	[2.1380 1.5912 3.3338 2.7681]	**1.18 0.075 0.384 0.43**
Mean Fading Power $\tilde{\Omega}$	20.0736 14.7808 30.8751 25.8691	20.0930 14.7907 30.8837 25.8604	**0.09 0.067 0.028 0.033**

Table: - 6.2.1 Comparison of different parameters for m=2.18

6.2.1) Simulated and Theoretical PDF for m=2.18 and m=2.5

The data sample used is 50000 and no. Of bins to obtain histogram of data used is 40.

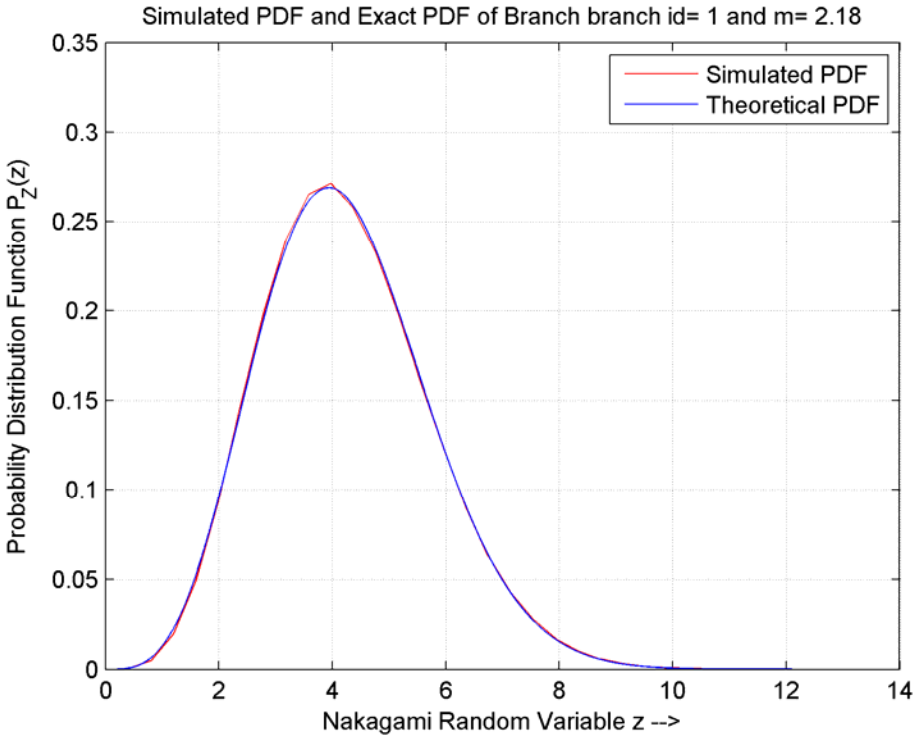

Figure 6.2.2 Simulated and Theoretical PDF for branch 1 and m=2.18

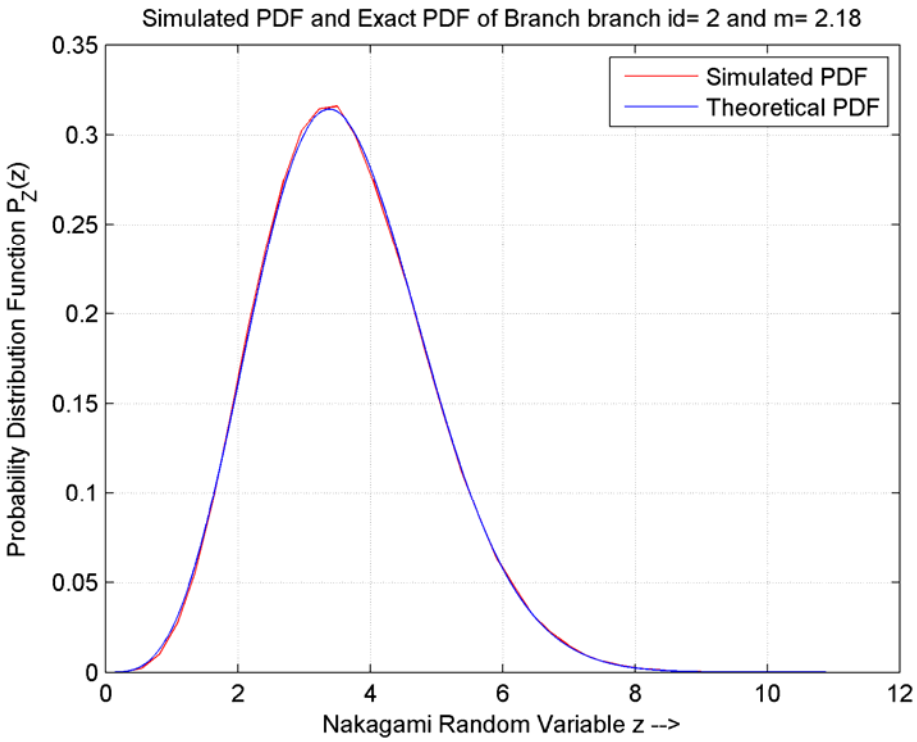

Figure 6.2.3 Simulated and Theoretical PDF for branch 2 and m=2.18

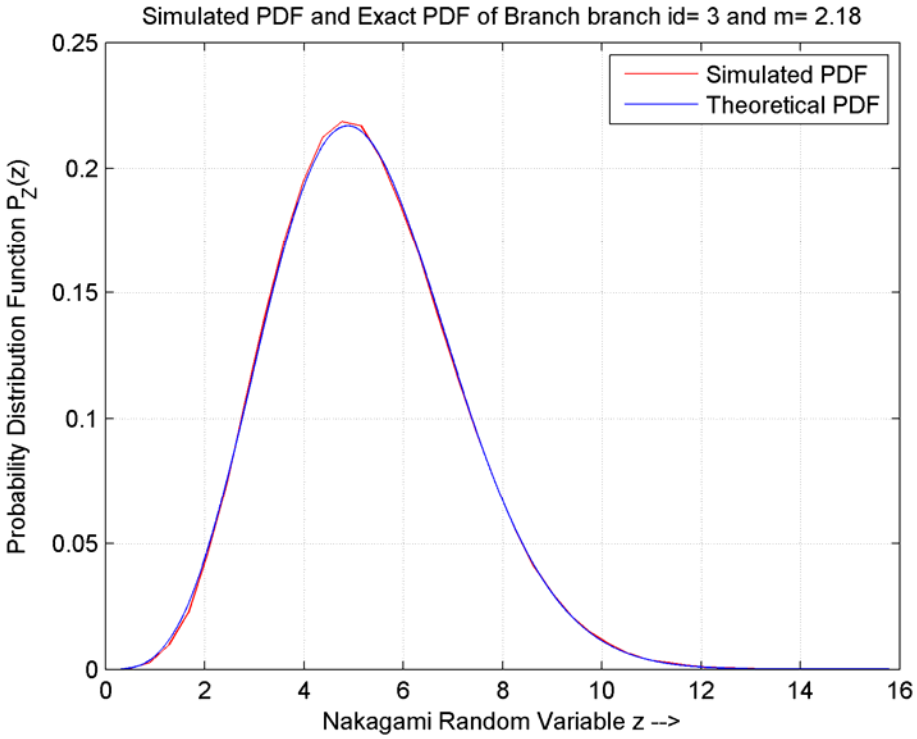

Figure 6.2.4 Simulated and Theoretical PDF for branch 3 and m=2.18

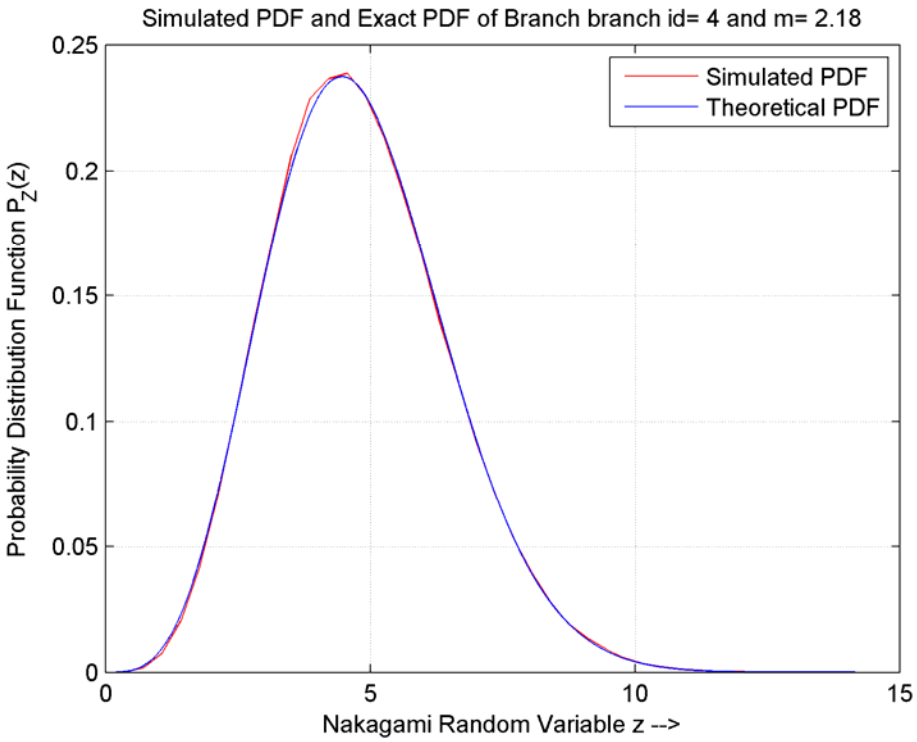

Figure 6.2.5 Simulated and Theoretical PDF for branch 4 and m=2.18

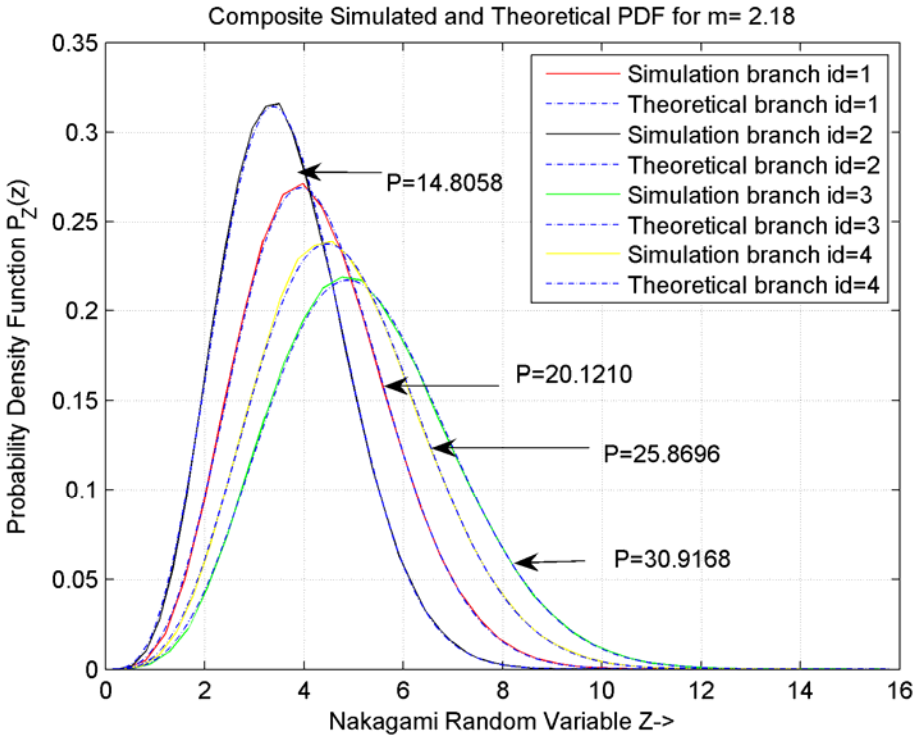

Figure 6.2.6 Composite Simulated and Theoretical PDF for m=2.18

Similar results have been obtained for m=2.5 which are given below.

Correlation coefficients for gamma vectors found out to be

v= [1.0000 0.8061 0.6178 0.3856]

And ς =**2.1145**

Estimated covariance matrix for Nakagami vector channel found out to be

$\tilde{R}_z$= **2.1539 1.4731 1.6195 0.9175**
1.4731 1.5853 1.8284 1.2727
1.6195 1.8284 3.3188 2.4268
0.9175 1.2727 2.4268 2.7857

Corresponding cross-correlation coefficients are

$\tilde{\rho}_z$ =**[1.0000 0.7972 0.6057 0.3746**]

And estimated variance vector is

$\tilde{P}_z$ = **[2.1539 1.5853 3.3188 2.7857]**

Parameter	**Theoretical Values**	**Practical Values**	**Error** (%)
Cross-Correlation Coefficients $\tilde{\rho}_z$	[1 0.795 0.604 0.372]	[1 0.7972 0.6057 0.3748]	**0.29 0.28 0.83**
Variance Vector $\tilde{P}_z$	[2.16 1.59 3.32 2.78]	[2.1539 1.5853 3.3188 2.757]	**0.28 0.296 0.036 0.74**
Mean Fading Power $\tilde{\Omega}$	22.8366 16.8102 35.1006 29.3915	22.8046 16.7947 35.0820 29.3898	**0.15 0.095 0.053 0.006**

Table 6.2.2 Comparison of different parameters for m=2.5

The following graphs show the simulated and theoretical results obtained for **m=2.5**

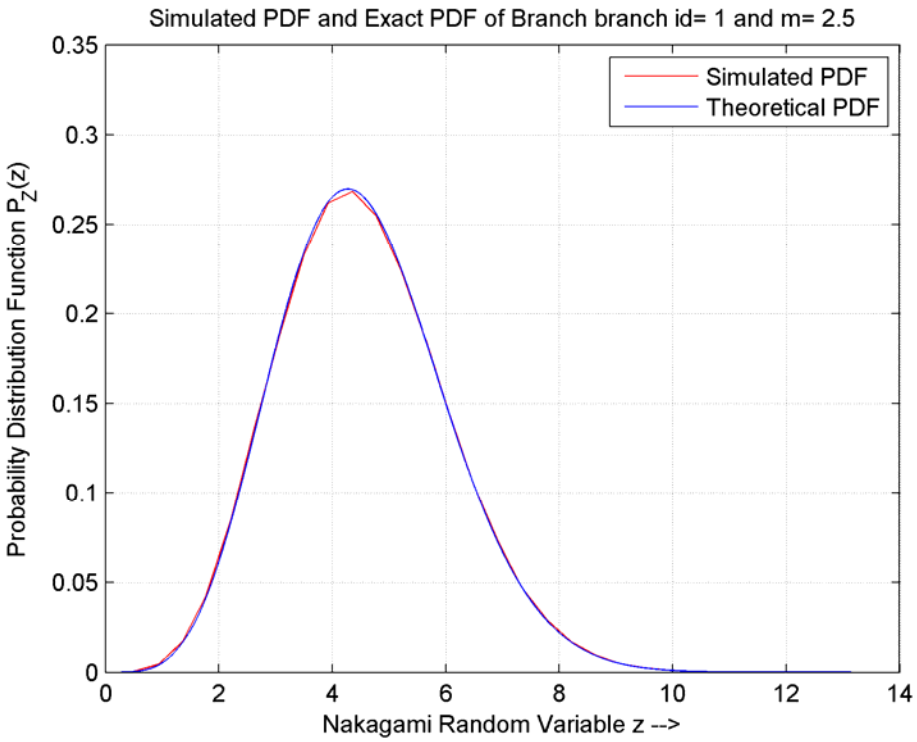

Figure 6.2.7 Simulated and Theoretical PDF for branch 1 and m=2.5

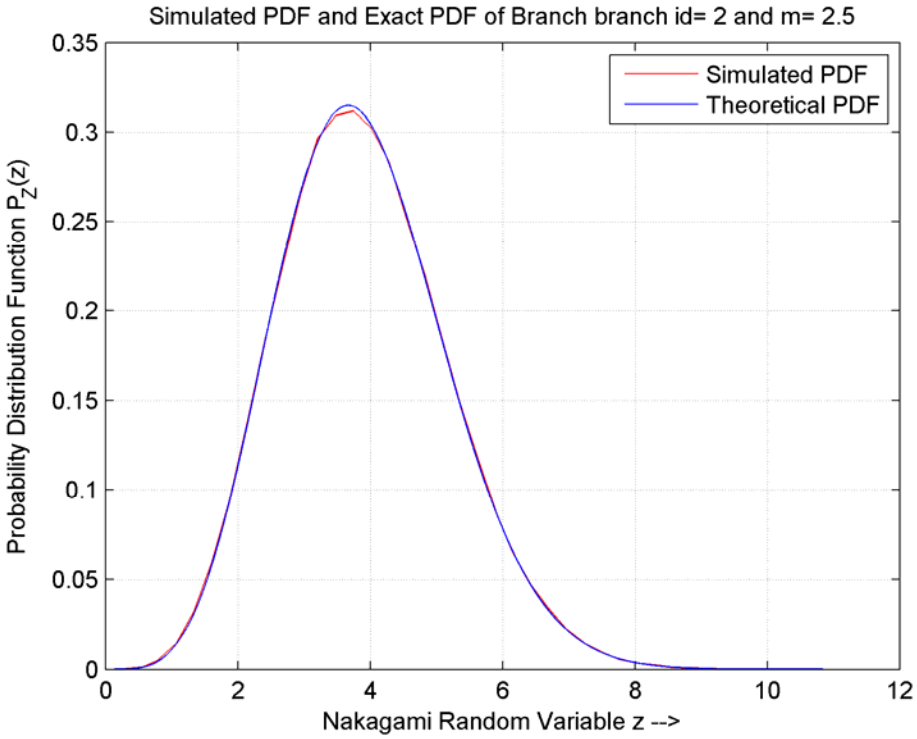

Figure 6.2.8 Simulated and Theoretical PDF for branch 2 and m=2.5

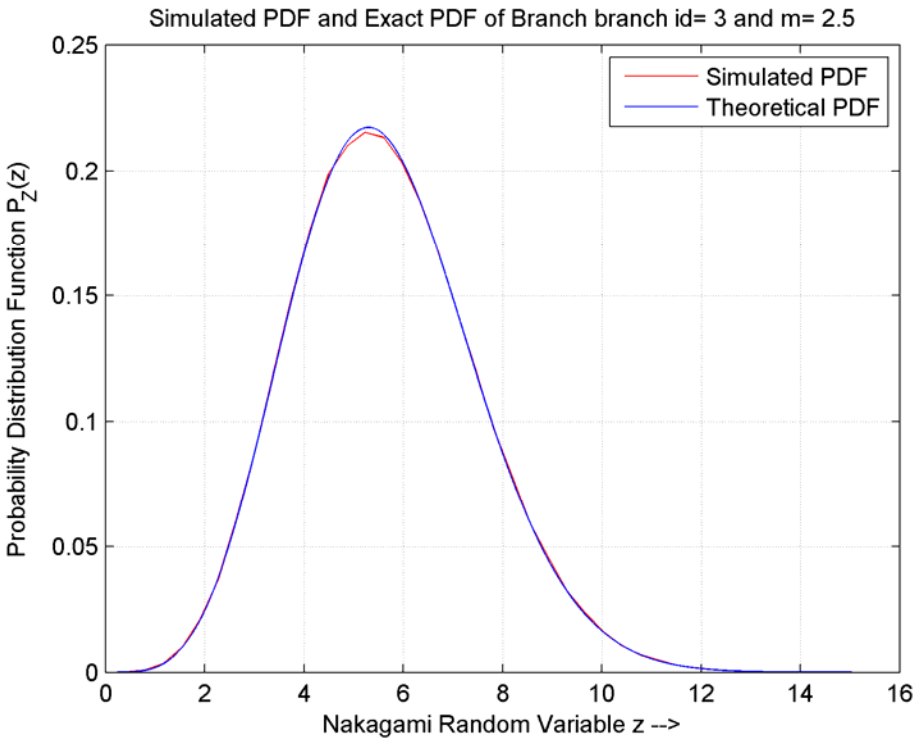

Figure 6.2.9 Simulated and Theoretical PDF for branch 3 and m=2.5

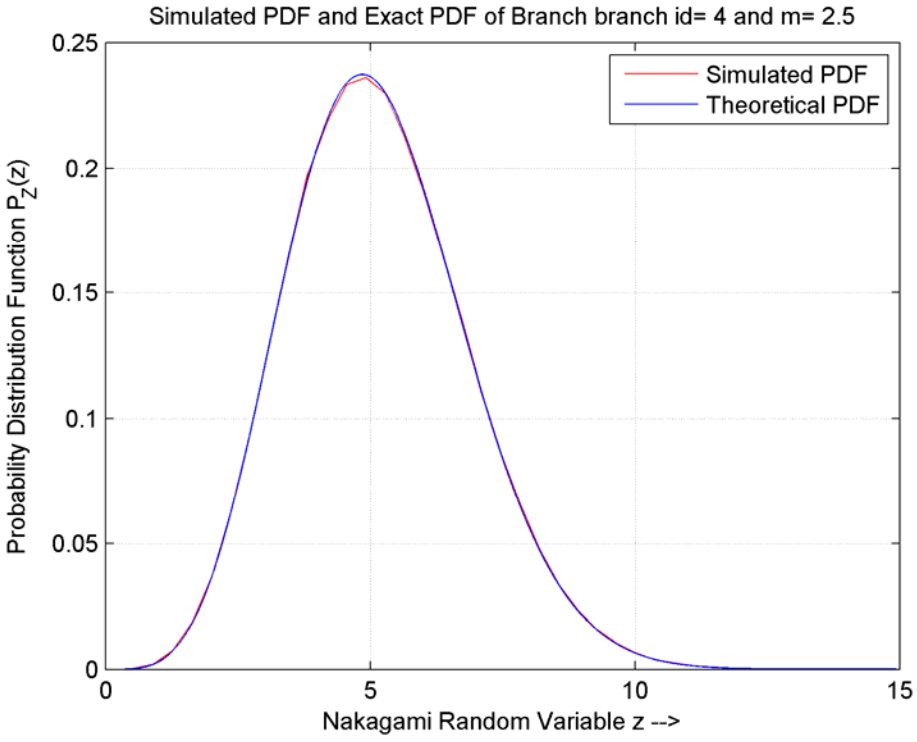

Figure 6.2.10 Simulated and Theoretical PDF for branch 4 and m=2.5

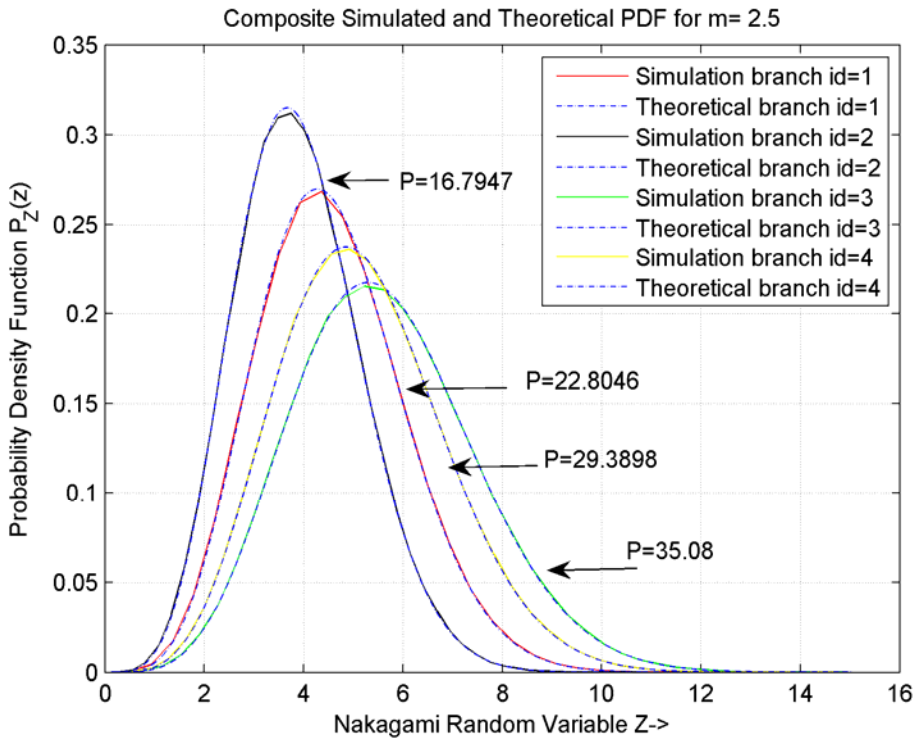

Figure 6.2.11 Composite Simulated and Theoretical for m=2.5

6.2.2) Discussions

- Simulated data using decomposition technique is in close agreement with theoretical probability density function for each branch
- The absolute percentage error in simulated and theoretical values for correlation coefficients is relatively small and even smaller for variance vectors. The same conclusion can be drawn for mean fading power.
- For the same fading parameter, Nakagami distribution moves towards right with increasing mean fading power and its maximum value is controlled by mean fading power which can be observed by figures (6.2.6) and (6.2.11).

CHAPTER 7

CONCLUSION AND SCOPE OF FUTURE WORK

In this thesis, we have seen the efficient sum of sinusoids method to generate Nakagami-m fading signal and its application to generate correlated vector fading channel for diversity application.

The idea used here is to represent correlated Nakagami vector as a non-linear function of a set of independent Gaussian vectors. We have also seen direct sum decomposition technique of determining covariance matrix of the Gaussian vectors from the specified covariance matrix of the Nakagami-m fading channel. In the original derivation fading parameter m is assumed to be multiple of ½. For m real, the decomposition expression consists of two parts, a principal factor and fine correction parameter. In the sum-of-sinusoids, we chose Improved Jake's Model to represent low pass Gaussian processes.

The theoretical and simulated PDF and autocorrelation appear to match well with small errors, which can be accounted for mismatch of first two moments. We can conclude from the received intensity plots that the fading is severe for m=0.5 and its severity reduces gradually as m increases leading to no fading condition when m approaches to ∞.

The Normalized autocorrelation have better match to its theoretical counterpart and it reaches unity when m approaches ∞. We have seen other higher order statistics like Level Crossing Rate and Average fade Duration. The simulation results provide excellent match with theoretical results. Furthermore the sum-of-sinusoids method along with direct sum

decomposition when applied to vector channels for diversity applications, found to deliver excellent match of theoretical and simulated probability density functions.

Future Research Work

The further research scope includes accurate simulation of continuous Nakagami-m phasor processes with arbitrary parameters and accurate statistics in terms of envelope, phase distribution and moments.

APPENDIX

A.1) Derivation of Level Crossing Rate N_R

The following equation represents Level Crossing Rate N_R at which envelope crosses a given level R in the positive direction

$$N_R = \int_0^\infty \dot{r}\, p(\dot{r}, r = R)\, d\dot{r} \tag{1}$$

Where $\dot{r}$ is a derivative of r with respect to time't'.

According to [15 equation 12], $p(\dot{r} \mid r) = \frac{1}{\sqrt{2\pi}\dot{\sigma}} \exp(-\frac{\dot{r}^2}{2\dot{\sigma}^2})$ Where

$$\dot{\sigma} = \beta v \sigma / \sqrt{2} \tag{2}$$

is a Standard Deviation of zero mean Gaussian distributed random variables.

The joint distribution of $\dot{r}$ and r is given by

$$p(\dot{r}, r) = p(\dot{r} \mid r)\, p(r) = \frac{1}{\sqrt{2\pi}\dot{\sigma}} \exp(-\frac{\dot{r}^2}{2\dot{\sigma}^2}) \frac{2}{\Gamma(m)} (\frac{m}{\Omega})^m r^{2m-1} \exp\{-\frac{mr^2}{\Omega}\} \tag{3}$$

Note that $p(\dot{r} \mid r)$ is independent of $p(\dot{r})$ and hence we can write

$$p(\dot{r}, r) = p(\dot{r})\, p(r) \tag{4}$$

Therefore $N_R = \int_0^\infty \dot{r}\, p(\dot{r}, r = R)\, d\dot{r} = \int_0^\infty \dot{r}\, p(\dot{r} \mid r)\, p(r)\, d\dot{r}$

$$N_R = p(r) \int_0^\infty \dot{r} \frac{1}{\sqrt{2\pi}\dot{\sigma}} \exp(-\frac{\dot{r}^2}{2\dot{\sigma}^2}) d\dot{r} = \frac{p(r)}{\sqrt{2\pi}\dot{\sigma}} \int_0^\infty \dot{r} \exp(-\frac{\dot{r}^2}{2\dot{\sigma}^2}) d\dot{r} \tag{5}$$

$\dot{r}^2 = t$ 2ṙdṙ = dt ṙdṙ = dt/2 Substituting in equation (4) we get

$$N_R = \frac{p(r)}{\sqrt{2\pi}\dot{\sigma}} \int_0^{\infty} \exp(\frac{-t}{2\dot{\sigma}^2}) dt / 2 = \frac{p(r)}{2\sqrt{2\pi}\dot{\sigma}} \left[\frac{\exp(\frac{-t}{2\dot{\sigma}^2})}{\frac{-1}{2\dot{\sigma}^2}} \right]_0^{\infty}$$

Solving above equation we get

$$N_R = \frac{\dot{\sigma}}{\sqrt{2\pi}} p(r) \tag{6}$$

$$N_R = \frac{\dot{\sigma}}{\sqrt{2\pi}} \left[\frac{2}{\Gamma(m)} (\frac{m}{\Omega})^m r^{2m-1} \exp\{-\frac{mr^2}{\Omega}\} \right]$$

$$\rho = \frac{R}{R_{rms}} = \frac{R}{\sqrt{\Omega}} \qquad \beta v = \frac{2\pi}{\lambda} v = 2\pi f_d$$

Define (7)

$$\sigma = \sqrt{\frac{\Omega}{2m}}$$

Combining equations (2) and (7) we get

$$\dot{\sigma} = \pi f_m \sqrt{\frac{\Omega}{m}} \tag{8}$$

Substituting equation (8) in equation (6) we get,

$$N_R = \frac{\pi f_d \sqrt{\frac{\Omega}{m}}}{\sqrt{2\pi}} \left[\frac{2}{\Gamma(m)} (\frac{m}{\Omega})^m r^{2m-1} \exp(-\frac{mr^2}{\Omega}) \right] \tag{9}$$

Solving equation (9) we get,

$$N_R = f_d \sqrt{2\pi} \left[\frac{1}{\Gamma(m)} (\frac{m}{\Omega})^{-1/2} (\frac{m}{\Omega})^m r^{2m-1} \exp(-\frac{mr^2}{\Omega}) \right] \tag{10}$$

From equation (7), we get $R = \rho\sqrt{\Omega}$

Substituting value of R in equation (10) and simplifying further we get Level Crossing Rate as

$$N_R = \frac{\sqrt{2\pi}\, f_d}{\Gamma(m)} \left(m\rho^2\right)^{m-1/2} \exp(-m\rho^2) \tag{11}$$

This is the closed form expression for Level Crossing Rate for Nakagami-m fading signal.

A.2) Derivation of Average Fade Duration T_R

The average fade duration T_R below r = R is given by

$$T_R = \frac{p[r \le R]}{N_R} = \frac{\int_0^R p(r)dr}{N_R} \tag{12}$$

$$\int_0^R p(r)dr = \frac{2}{\Gamma(m)} m^m \int_0^R \frac{r^{2m-1}}{\Omega^m} \exp(-\frac{mr^2}{\Omega})dr \tag{13}$$

Let $\frac{r}{\Omega^{1/2}} = z$ $\qquad dr = \Omega^{1/2} dz$ $\qquad \frac{r^2}{\Omega} = z^2$

And corresponding integral limits are

$r -> R$ $\qquad z = \frac{R}{\sqrt{\Omega}} = \rho$

$r -> 0$ $\qquad z = 0$

Equation (13) becomes,

$$p(r) = \frac{2}{\Gamma(m)} m^m \int_0^\rho \frac{\left(z\sqrt{\Omega}\right)^{2m-1}}{\Omega^m} \exp(-mz^2) dz\sqrt{\Omega} \tag{14}$$

Simplifying Equation (14) we get,

$$p(r) = \frac{2}{\Gamma(m)} m^m \int_0^{\rho} z^{2m-1} \exp(-mz^2) dz \tag{15}$$

Define $\psi(m, \rho) = \int_0^{\rho} z^{2m-1} \exp(-mz^2) dz$ (16)

Thus equation (15) becomes

$$p(r) = \frac{2}{\Gamma(m)} m^m \psi(m, \rho) \tag{17}$$

Substituting equation (17) and (11) in equation (12) we get

$$T_R = \frac{\frac{2}{\Gamma(m)} m^m \psi(m, \rho)}{\frac{\sqrt{2\pi} f_d}{\Gamma(m)} \left(m\rho^2\right)^{m-1/2} \exp(-m\rho^2)}$$

After simplification, we get closed form expression for AFD as

$$T_R = \frac{2\sqrt{m}\psi(m, \rho)}{\sqrt{2\pi} f_d \rho^{2m-1} \exp(-m\rho^2)} \tag{18}$$

This is the closed form expression for Average Fade Duration for Nakagami-m fading signal.

REFERENCES

[1] M. Nakagami, "The m-distribution- a general formula of intensity distribution of rapid fading", in statistical methods in Radio Wave propagation, W.C. Hoffman, Ed. New York: Pergamon, 1960 pp: 3-36

[2] Q. T. Zhang, "A Decomposition technique for efficient generation of correlated Nakagami Fading Channels

[3] K. Zhang, Z. F. Song, and Y. L. Guan, "Simulation of Nakagami fading channels with arbitrary cross-correlation and fading parameters," IEEE Trans. Wireless Commun. Vol. 3, no. 5, pp. 1463–1468, Sept. 2004.

[4] N. C. Beaulieu and C. Cheng, "An efficient procedure for Nakagami-m fading simulation," Proc. IEEE GLOBECOM, pp. 3336–3342, Nov. 2001.

[5] http://people.deas.harvard.edu/~jones/es151/prop_models/propagation.html

[6] Y. Chen and N. C. Beaulieu, "Estimation of Rician and Nakagami distribution parameters using noisy samples," IEEE Int. Conf. on Commun. (ICC), June 2004.

[7] C. Tepedelenlioglu and G. Ping, "Practical issues in the estimation of Nakagami-m parameter," Proc. IEEE GLOBECOM, vol. 2, pp. 972–976, 2003.

[8] J. Cheng and N. C. Beaulieu, "Generalized moment estimators for the Nakagami fading parameter," IEEE Commun. Lett. Vol. 6, pp. 144–146, Apr. 2002.

[9] Lingzhi Cao; Beaulieu, N.C.; "A simple efficient procedure for generating bivariate Nakagami-m fading samples" Communications, 2005. ICC 2005. 2005

IEEE International Conference on Commun. Volume 2, 16-20 May 2005 Page(s): 886 - 889 Vol. 2

[10] R. B. Ertel and J. H. Reed, "Generation of correlated Rayleigh fading envelopes" IEEE commun. lett. Vol. 3 pp, 276-278, Oct 1998.

[11] Zhang Q. T. "Correlated Nakagami Fading Channels with different fading parameters: A generic characterization with Application," Communications, 2002. ICC 2002. IEEE International Conference on Volume 2, 28 April-2 May 2002 Page(s): 704 - 708 vol.2

[12] K.W. Yip and T.S. Ng, "A simulation model for Nakagami-m fading channels, $m \leq 1$," IEEE Trans. Commun. vol. 48, no. 2, pp. 214–221, Feb. 2000.

[13] Norman C. Beaulieu and C. Cheng, "Efficient Nakagami- m Fading Channel Simulation," IEEE trans. on vehicular Tech. vol.54 no.2, pp. 413-424 March 2005

[14] Tsan-Ming Wu, Shiuna-Yuan Tzeng, "Sum-of-sinusoids based simulator for Nakagami-m fading channels" Vehicular Tech. Conf. 2003, VTC 2003-Fall IEEE 58th vol. 1, 6-9 Oct 2003 Page(s): 158-162

[15] Yacoub, M.D.; Bautistu, J.E.V.; Guerra de Rezende Guedes, L.; "On higher order statistics of the Nakagami-m distribution" Vehicular Technology, IEEE Transactions Volume 48, Issue 3, May 1999 Page(s): 790 – 794

[16] Iskander, C.D.; Takis Mathiopoulos, P., "Analytical level crossing rates and average fade durations for diversity techniques in Nakagami fading channels," Communications, IEEE Transactions on Volume 50, Issue 8, Aug. 2002 Page(s): 1301 – 1309

[17] http://people.deas.harvard.edu/~jones/es151/prop_models/propagation.html

[18] R.H. Clarke, "A statistical theory of mobile-radio propagation," Bell Syst. Tech. pp 957-1000 July-August 1968

[19] I. S. Gradshteyn, I. M. Ryzbik, "Tables of Integrals, Series and Products," Edition 6th Academic Press 2000

[20] J. G. Proakis, Digital Communications, and 4th Edition New York: McGraw-Hill 2001

[21] W. C. Lee, Mobile Communications: Design Fundamentals, 2nd Ed. New York: Wiley, 1993 PP.202-211

[22] M. F. Pop and N. C. Beaulieu, "Limitations of sum-of-sinusoids fading channel simulators," IEEE. Trans. Commun. Vol. 49 no.4 pp.699-708 April 2001

[23] http://philsci-archive.pitt.edu/archive/00002412/01/Simulations.pdf